Taphonomy and taxonomy of a juvenile lambeosaurine (Ornithischia: Hadrosauridae) bonebed from the late Campanian Wapiti Formation of northwestern Alberta, Canada

Brayden Holland [Corresp., 1], **Phil R Bell** [1], **Federico Fanti** [2], **Samantha Hamilton** [3], **Derek W Larson** [4], **Robin Sissons** [3], **Corwin Sullivan** [3, 4], **Matthew J Vavrek** [5], **Yanyin Wang** [3], **Nicolás E Campione** [Corresp. 1]

[1] Palaeoscience Research Centre, School of Environmental and Rural Science, University of New England, Armidale, New South Wales, Armidale

[2] Dipartimento di Scienze Biologiche, Geologiche e Ambientali, Alma Mater Studiorum, Università di Bologna, Bologna, Italy

[3] Department of Biological Sciences, University of Alberta, Edmonton, Alberta, Canada

[4] Philip J. Currie Dinosaur Museum, Wembley, Alberta, Canada

[5] Department of Natural History, Royal Ontario Museum, Toronto, Ontario, Canada

Corresponding Authors: Brayden Holland, Nicolás E Campione
Email address: blongle2@myune.edu.au, ncampion@une.edu.au

Hadrosaurid (duck-billed) dinosaur bonebeds are exceedingly prevalent in upper Cretaceous (Campanian–Maastrichtian) strata from the Midwest of North America (especially Alberta, Canada, and Montana, U.S.A) but are less frequently documented from more northern regions. The Wapiti Formation (Campanian–Maastrichtian) of northwestern Alberta is a largely untapped resource of terrestrial palaeontological information missing from southern Alberta due to the deposition of the marine Bearpaw Formation. In 2018, the Boreal Alberta Dinosaur Project rediscovered the Spring Creek Bonebed, which had been lost since 2002, along the northern bank of the Wapiti River, southwest of Grande Prairie. Earlier excavations and observations of the Spring Creek Bonebed suggested that the site yielded young hadrosaurines. Continued work in 2018 and 2019 recovered ~300 specimens that included a minimum of eight individuals, based on the number of right humeri. The morphology of several recovered cranial elements unequivocally supports lambeosaurine affinities, making the Spring Creek sample the first documented occurrence of lambeosaurines in the Wapiti Formation. The overall size range and histology of the bones found at the site indicate that these animals were uniformly late juveniles, suggesting that age segregation was a life history strategy among hadrosaurids. Given the considerable size attained by the Spring Creek lambeosaurines, they were probably segregated from the breeding population during nesting or caring for young, rather than due to different diet and locomotory requirements. Dynamic aspects of life history, such as age segregation, may well have contributed to the highly diverse and cosmopolitan nature of Late Cretaceous hadrosaurids.

Taphonomy and taxonomy of juvenile lambeosaurine (Ornithischia: Hadrosauridae) bonebed from the late Campanian Wapiti Formation of northwestern Alberta, Canada

Brayden Holland[1], Phil R. Bell[1], Federico Fanti[2], Samantha M. Hamilton[3], Derek W. Larson[4], Robin L. Sissons[3], Corwin Sullivan[3, 4], Matthew J. Vavrek[5], Yan-Yin Wang[3], Nicolás E. Campione[1]

[1]Palaeoscience Research Centre, School of Environmental and Rural Science, University of New England, Armidale, NSW, Australia

[2] Dipartimento di Scienze Biologiche, Geologiche e Ambientali, Alma Mater Studiorum, Università di Bologna, Bologna, Italy

[3]Department of Biological Sciences, University of Alberta, Edmonton, AB, Canada

[4]Philip J. Currie Dinosaur Museum, Wembley, AB, Canada

[5]Department of Natural History, Royal Ontario Museum, Toronto, ON, Canada

Corresponding Authors:

Brayden Holland and Nicolás E. Campione

University of New England, Armidale, NSW, 2351, Australia

Email address: blongle2@myune.edu.au; ncampion@une.edu.au

Abstract

Hadrosaurid (duck-billed) dinosaur bonebeds are exceedingly prevalent in upper Cretaceous (Campanian–Maastrichtian) strata from the Midwest of North America (especially Alberta, Canada, and Montana, U.S.A) but are less frequently documented from more northern regions. The Wapiti Formation (Campanian–Maastrichtian) of northwestern Alberta is a largely untapped resource of terrestrial palaeontological information missing from southern Alberta due to the deposition of the marine Bearpaw Formation. In 2018, the Boreal Alberta Dinosaur Project rediscovered the Spring Creek Bonebed, which had been lost since 2002, along the northern bank of the Wapiti River, southwest of Grande Prairie. Earlier excavations and observations of the Spring Creek Bonebed suggested that the site yielded young hadrosaurines. Continued work in 2018 and 2019 recovered ~300 specimens that included a minimum of eight individuals, based on the number of right humeri. The morphology of several recovered cranial elements unequivocally supports lambeosaurine affinities, making the Spring Creek sample the first documented occurrence of lambeosaurines in the Wapiti Formation. The overall size range and histology of the bones found at the site indicate that these animals were uniformly late juveniles, suggesting that age segregation was a life history strategy among hadrosaurids. Given the considerable size attained by the Spring Creek lambeosaurines, they were probably segregated from the breeding population during nesting or caring for young, rather than due to different diet and locomotory requirements. Dynamic aspects of life history, such as age segregation, may well have contributed to the highly diverse and cosmopolitan nature of Late Cretaceous hadrosaurids.

Introduction

Macrofossil bonebeds are a source of palaeontological data that greatly contribute to our understanding of anatomy, diversity, life history, community structure, behaviour, population dynamics, and taphonomy (Rogers et al., 2007). In North America, hadrosaurid dinosaur bonebeds are particularly concentrated in uppermost Cretaceous (Campanian–Maastrichtian) deposits, notably in those of the Belly River and Edmonton groups in southern Alberta, Canada (Getty et al., 1998; Eberth & Getty, 2005; Eberth & Currie, 2010; Bell & Campione, 2014; Eberth, 2015; Evans et al., 2015) and the Two Medicine, Hell Creek, Lance, and Judith River formations in the northern part of the western United States (Christians, 1992; Varricchio & Horner, 1993; Britt et al., 2009; Scherzer & Varricchio, 2010; Keenan & Scannella, 2014; Prieto-Márquez & Gutarra, 2016). Hadrosaurid specimens from bonebeds in these formations were among the first dinosaurs to be histologically sampled, which allowed for the reconstruction of their growth rates (Horner & Currie, 1994; Horner et al., 1999, 2000) and provided the first evidence for parental care in dinosaurs (Horner & Makela, 1979; Horner et al., 2000). Despite their frequency and importance, large numbers of North American hadrosaurid bonebeds have not been described in detail, particularly in northern rock units such as the Wapiti Formation (Fanti & Catuneanu, 2009; Fanti & Miyashita, 2009). These offer the opportunity to explore the diversity and preservation of hadrosaurids outside the traditionally sampled North American strata.

In northwestern Alberta, Wapiti Formation deposits span the mid-Campanian to upper Maastrichtian and are contemporaneous with most of the Belly River and Edmonton groups in southern Alberta (Fanti & Catuneanu, 2009; Eberth & Braman, 2012). Unlike its more famous southern counterparts, which are interrupted by marine transgressions of the Bearpaw Formation,

the Wapiti Formation is a continuous package of terrestrial sediments (Eberth & Getty, 2005; Fanti & Catuneanu, 2009; Eberth & Braman, 2012). Although the Wapiti Formation was originally well-known only for a single ceratopsian site, the Pipestone Creek Bonebed (Currie et al., 2008a), fieldwork over the past 10–15 years has uncovered abundant vertebrate ichnofossils (Bell et al., 2013; Fanti et al., 2013), articulated skeletons with skin impressions (Bell et al., 2014a; Bell et al., 2014b), microfossil sites (Fanti & Miyashita, 2009), and macrofossil bonebeds (Tanke, 2004; Currie et al., 2008a; Fanti et al., 2015) (Fig. 1).

The Pipestone Creek Bonebed was discovered in 1974 (Tanke, 2004) and has produced disarticulated bones representing at least 27 juvenile- to adult-sized individuals of the ceratopsian *Pachyrhinosaurus lakustai*, along with remains of the dromaeosaurid *Boreonykus certekorum*, tyrannosaurids, and non-dinosaurian vertebrates (Currie et al., 2008a; Bell & Currie, 2016). Its unique faunal content has been used to support dinosaur endemism hypotheses across Laramidia during the Late Cretaceous (Currie et al., 2008a; Sampson et al., 2010; Lucas et al., 2016). The Wapiti River Bonebed, a second ceratopsian bonebed located west of the Pipestone Creek Bonebed, is dominated by *Pachyrhinosaurus* specimens that have not yet been conclusively identified at the species level. Notably, this bonebed represents one of the most inland occurrences of centrosaurine ceratopsians in North America, given its inferred location relative to the Western Interior Seaway (Fanti et al., 2015). In addition to macrofossil bonebeds (defined as >75% of specimens with a preserved length >5 cm; sensu Eberth et al., 2007a), the Kleskun Hill microfossil site (defined as >75% of specimens with a preserved length <5 cm) preserves a high diversity of vertebrates, including fish, lizards, dinosaurs, and mammals (Fanti & Miyashita, 2009). Several additional monodominant hadrosaurid bonebeds have subsequently

been discovered, although not yet documented in detail (Tanke, 2004; Bell et al., 2014a; Bell et al., 2014b).

The hadrosaurids of the Wapiti Formation are taxonomically enigmatic. *Edmontosaurus regalis* is currently the only species reported from this temporally extensive formation (Bell et al., 2014a; Bell et al., 2014b). The majority of hadrosaurid material so far recovered came from Unit 4 of the formation, which is broadly contemporaneous with portions of the Horseshoe Canyon Formation of southern Alberta, from which *E. regalis* is commonly recovered (Bell et al., 2014a; Bell et al., 2014b; Campione & Evans, 2011; Eberth et al., 2013). Moreover, there is yet to be any definitive evidence to suggest the presence of another hadrosaurid taxon beside *E. regalis* in Unit 4. However, it is unlikely that *E. regalis* was the only hadrosaurid from the entire formation, given the known diversity of hadrosaurids elsewhere in Alberta and the temporal extent of the Wapiti Formation. For instance, lambeosaurines have yet to be documented from the formation, despite their ubiquity within both the Belly River and Edmonton groups (Lull & Wright, 1942; Evans et al., 2005; Ryan & Evans, 2005; Evans & Reisz, 2007; Evans et al., 2007; Evans, 2010; Brink et al., 2011; Mallon et al., 2012; Eberth et al., 2013; Farke et al., 2013).

In 1988, Grande Prairie Regional College staff discovered several well-preserved hadrosaurid bones along the northern bank of the Wapiti River, approximately 150 m downstream of the confluence with the Spring Creek (Tanke, 2004). The site was dubbed the Spring Creek Bonebed (SCBB), and the material was suggested to possibly pertain to Hadrosaurinae, based on the “low deltoid crests” morphology seen in the recovered humeri. Given their size range, the bones were interpreted as the remains of subadult individuals that may have formed a “bachelor herd” (Tanke, 2004). Initial excavations at the SCBB undertaken by Grande Prairie Regional College and Royal Tyrrell Museum began in 1988, resulting in 40

specimens recovered between 1988 and 2002. By 2003, however, the site had been obscured by riverbank slumping (Tanke, 2004) and could not be rediscovered despite repeated attempts over the following years. The bonebed was finally rediscovered in 2018 by one of us (MJV) as part of the Boreal Alberta Dinosaur Project and subsequently excavated during the 2018 and 2019 field seasons (Fig. 2). These recent excavations secured hundreds of new hadrosaurid specimens, including the first diagnostic cranial material.

In this study, we describe the anatomy of the most taxonomically informative hadrosaurid bones preserved at the SCBB and examine the taphonomic factors that may have formed the bonebed. We test the original suggestion that the material might belong to Hadrosaurinae (Tanke, 2004) using a larger sample that encompasses more diagnostic elements and use histological analyses to assess the age distribution of the bonebed sample. Finally, we consider the nature of fossil deposition at the SCBB, with a particular focus on whether the bonebed assemblage originated through attrition or mass mortality, and explore the implications for how hadrosaurid life histories should be envisaged.

Geological setting

Outcrops of the terrestrial Wapiti Formation are exposed extensively in central to northwestern Alberta (Fig. 1) and into the eastern-most regions of British Columbia. Stratigraphically, the Wapiti Formation overlies the marine Puskwaskau Formation and underlies the terrestrial Scollard Formation (Fanti & Catuneanu, 2009). Spanning from the mid-Campanian (~79.1 Ma) into the Maastrichtian (~67 Ma), the Wapiti Formation is roughly contemporaneous with the Belly River and Edmonton groups of southern Alberta and the Two Medicine and St.

Mary River formations of northwestern Montana (Fanti & Catuneanu, 2010; Eberth & Kamo, 2020; Zubalich et al., 2021). The formation is subdivided into five units that suggest an overall progression from channel-fill sandstones to floodplain-derived finer sediments (Fanti & Catuneanu, 2009, 2010). Importantly, coals from Unit 3 and the Red Willow coal zone (upper Unit 4) are interpreted as synchronous with the maximum flooding surfaces of the marine Bearpaw Formation and Drumheller Marine Tongue, respectively (Fanti & Catuneanu, 2009). However, actual marine sediments do not interrupt the succession of terrestrial strata in this region, as they do in southern Alberta. Therefore, the Wapiti Formation represents a nearly continuous mid-Campanian–Maastrichtian terrestrial record that is important for tracking faunal transformation in northern Laramidia, particularly when marine transgressions inundated southern Alberta.

Because the Wapiti Formation exposures in which the SCBB is located are highly unstable and prone to slumping, the stratigraphic position of the bonebed is limited to within a few metres. The SCBB is located ~11.5 km downstream of the Pipestone Creek Bonebed, placing it within Unit 3 of the Wapiti Formation and implying rough contemporaneity with the lowermost units of the Horseshoe Canyon Formation (the Strathmore and Drumheller members: Currie et al., 2008b; Eberth & Braman, 2012; Zubalich et al., 2021). Unit 3 comprises channel sandstones overlain by interbedded mudstones and siltstones, minor sandstone sheets, and extensive coals, representing fluvial point bars within high-sinuosity fluvial systems in floodplain environments (Fanti & Catuneanu, 2009). At the SCBB locality (Fig. 3), approximately 14 vertical metres of the Wapiti Formation are exposed on a cut bank of the Wapiti River, where slumping has obscured some sedimentary features and the boundaries between horizons. Nevertheless, massive mudstones up to 5.5 m thick (interrupted by thin sandy

154 layers) dominate the exposure, alternating with sandstones up to 2.8 m thick (Fig. 3). The SCBB
155 is confined to a ~40 cm thick horizon within the middle of a massive, organic-rich mudstone
156 approximately 3.7 m thick. Bones exhibit no signs of grading, range from 10 to 640 mm in
157 maximum length, and have no distinct preferred orientation (see Results). In addition to bones,
158 coalified plant remains (< 10 cm long), clay nodules, and amber (< 2 cm long) are also present in
159 the bonebed. Conformably underlying the bonebed-hosting mudstone is a ~80 cm thick
160 sandstone with shallow crossbedding, which overlies a coal layer that is only exposed during low
161 water periods. The overall sedimentary evidence indicates the SCBB was deposited on a
162 vegetated floodplain traversed by the meandering rivers that were the main depositional
163 environment for Unit 3 (Fanti & Catuneanu, 2009).

164

165 Materials & Methods

166 Excavation

167 Specimens collected by the Grande Prairie Regional College in 1988 and 1991 were
168 mapped but could not be placed in our quarry maps or used in our quarry analyses because
169 accompanying orientation data, field identifications, and field numbers were not recorded.
170 During the Boreal Alberta Dinosaur Project excavations in 2018 and 2019, orientation, plunge,
171 and maximum preserved length were recorded on-site for all specimens with a length:width ratio
172 ≥ 2. Obvious taphonomic artefacts, such as fracturing, were noted. All specimens with a total
173 length > 5 cm were mapped by hand in 1 x 1 m grids, subdivided into 10 x 10 cm squares.
174 Specimens collected in 1988 and 1991 are accessioned at the Royal Tyrrell Museum of
175 Palaeontology (TMP), Drumheller, Alberta, Canada (TMP1988.094 and TMP1991.137 series),

whereas specimens collected in 2018 and 2019 are accessioned in the collections of the University of Alberta's Laboratory for Vertebrate Palaeontology (UALVP), Edmonton, Alberta, Canada.

Histology

For consistency, we followed the methods and definitions used in previous histological studies of hadrosaurids (Horner et al., 1999; Horner et al., 2000; Vanderven et al., 2014; Woodward et al., 2015, Wosik et al., 2020). We sectioned the eight most complete humeri along the diaphysis (distal to the deltopectoral crest), as they offer the best sampled and most readily prepared bone from the bonebed (Fig. 4; Table 1). Humeri were chosen because they form the basis for MNI, guaranteeing that histological comparisons are performed on distinct individuals and approximating the relative age in the assemblage. Although humeri have been used in multiple hadrosaurid histological analyses (Horner et al., 2000; Vanderven et al., 2014; Wosik et al., 2020), future studies could sample yet-to-be-prepared tibiae and femora, to better constrain the absolute ages of these hadrosaurids (Horner et al., 1999; Horner et al., 2000; Vanderven et al., 2014; Woodward et al., 2015, Wosik, et al., 2020).

Thin sections of TMP specimens were produced at the University of New England (Australia), and thin sections of UALVP specimens were produced at the University of Alberta (Canada). Humeri sectioned at the University of New England were partially encased in epoxy resin to minimize damage during sectioning. The sections were cut using a diamond saw, before being mounted on slides and hand-polished with 600 grit silicon carbide. Slides were then placed into a Petrothin thin sectioning machine and ground down to 200 μm. The slides were then

placed into a Logitech LP50 polisher to be ground down to 30 µm. Sections were analyzed under 10X magnification on a Leica DM500 compound microscope and were photographed under LED lighting with a Canon EOS 5DS.

Humeri prepared at the University of Alberta were sectioned at mid-diaphysis using a table saw. Sections were then placed into plastic containers before being covered by EAGER Polymers' EP4101UV Crystal Clear Polyester Resin (Castolite AP & Castolite AC) and EP4920 MEK-P Castolite Hardener (mixed in a 1 oz: 10 drops volume ratio). The cured resin blocks were cut in half using a table saw and mounted on plexiglass slides. Prior to mounting, both the plexiglass slides and resin blocks were faced using 1000 grit silicon carbide grinding mixture. The sections were then ground down on a Hillquist saw using 600 and 1000 grit grinding mixtures until suitable transparency, rather than any predefined thickness, was achieved. Images were captured under 4X magnification using a Nikon DS-FI3 camera, mounted on a Nikon Eclipse E600 POL microscope, and Nikon NIS Elements (v. 4.60) imaging software housed in the Caldwell Lab, University of Alberta.

Taphonomy

All specimens were identified and inspected for taphonomic and preparation artefacts following laboratory preparation. Taphonomic analyses follow the procedures outlined by Behrensmeyer (1991) and built upon by Eberth et al. (2007a) and Blob and Badgley (2007). Taphonomic parameters were broadly categorized into either assemblage, quarry, or bone modification data, and analyzed under subcategories as outlined by Behrensmeyer (1991). In this study, a specimen is defined as a vertebrate hard part (e.g., bone, tooth, scale) regardless of possible association

with another bone (Blob & Badgley, 2007). Accordingly, multiple fused bones represent a single specimen, whereas unfused, but associated, bones (e.g., a string of vertebrae) are counted individually as distinct specimens. An element is defined as a vertebrate hard part in its entirety, such as a complete tibia as opposed to a distal piece of a tibia (Badgley, 1986; Blob & Badgley, 2007). A broken, but matchable element (e.g. a femur broken into four pieces, or distal and proximal ends of a femur) is regarded as a single specimen if the pieces can be reassembled. Analyses of taphonomic data utilized the total number of specimens (N), the number of identifiable specimens (NISP), and the number of prepared specimens (NPSP). The NISP is larger than the NPSP because few prepared specimens could not be identified. Except where noted, bone modification data are based on the NPSP, whereas assemblage and quarry data are based on the NISP. The minimum number of individuals (MNI) was determined by counting the most common unique skeletal elements (Blob & Badgley, 2007), which in the case of the SCBB were right humeri (Fig. 4; Table 1).

Voorhies (1969) groups are commonly used to assess skeletal representation and fluvial influence in bonebeds (Gangloff & Fiorillo, 2010; Bell & Campione, 2014; Evans et al., 2015). However, their application to large-bodied extinct taxa has been questioned (Eberth et al., 2007a; Britt et al., 2009; Peterson et al., 2013), as Voorhies groups do not account for bone completeness and disarticulation, particularly of the skull, prior to transportation. Additionally, Voorhies groups were originally used to examine the taphonomy of skeletally fused mammals rather than reptiles. Such factors can cause inaccurate element counts, leading to incorrect ratios between Voorhies groups and false inferences regarding fluvial influence, but elements can be counted more accurately by accounting for the lack of skeletal fusion in younger hadrosaurids (Horner & Currie, 1994). Moreover, the relative proportion of element representation is more

243 informative than absolute counts (Gangloff & Fiorillo, 2010; Bell & Campione, 2014). For this
244 study, Voorhies groups are based on inferred susceptibility to transport given a specimen's size
245 (as redefined by Scherzer & Varricchio, 2010; Varricchio, 1995), and the expected numbers of
246 each element in a single hadrosaurid skeleton were derived from Horner et al. (2004) and Bell
247 and Campione (2014) (Table 2).

248 Age class designation follows two criteria. The first is that of Horner (2000), who
249 identified six classes based on histology: early and late nestling, early and late juvenile, sub-
250 adult, and adult. When histological data are not available, we follow the size-based criterion used
251 by Evans (2010), in which individuals beyond perinatal size and yet to attain 50% of adult size
252 are defined as juvenile.

253

254 Results

255 Anatomical descriptions

256 The most diagnostic elements recovered from the SCBB include a premaxilla, maxilla,
257 and postorbital, all of which show unambiguous lambeosaurine affinities. These elements are
258 described in detail below.

259 *Premaxilla*—A partial left premaxilla (UALVP 60537) is preserved in two equal-length
260 but non-contiguous pieces, separated by a gap of several millimetres (Fig. 5). Most of the
261 anterior region of the premaxilla is intact, revealing the facial angle and the shape of the bill.
262 However, the posterior contact with the nasal is absent, as is most of the premaxillary
263 contribution to the cranial crest.

264 The oral margin of the premaxilla is rugose and was likely covered by a keratinous
265 rhamphotheca in life (Morris, 1970; Horner et al., 2004; Farke et al., 2013). In dorsal view, the
266 oral margin is transverse anteriorly and broadly arcuate more posteriorly with a smooth transition
267 to the post-oral region of the premaxilla. As a result, it does not form a distinct, ventrolaterally
268 directed tab-like process, as seen in other juvenile lambeosaurines (such as *Hypacrosaurus*,
269 *Parasaurolophus*, and *Velafrons coahuilensis*; Gates et al., 2007; Evans, 2010; Brink et al.,
270 2011), although the development of this process varies ontogenetically in lambeosaurines (Table
271 3; Evans, 2010). The anterior third of the preserved length of the premaxilla's dorsal surface is
272 concave mediolaterally, corresponding to the contour of the bony naris. The preserved bony naris
273 has a length:width ratio of 3.5, exceeding the ratio observed in the southern Laramidian taxa
274 *Magnapaulia laticaudus* and *V. coahuilensis* (1.85–2.85; Prieto-Márquez et al., 2012), though
275 this is likely due to ontogeny (Prieto-Márquez et al., 2012). The bony naris attenuates anterior to
276 the crest-snout angle, similar to juvenile *Lambeosaurus lambei, V. coahuilensis* and
277 *Hypacrosaurus altispinus* (Lull & Wright, 1942; Ostrom, 1961; Evans et al., 2005; Gates et al.,
278 2007; Evans, 2010), but in contrast to the more posterior attenuated bony naris seen in juvenile
279 *Corythosaurus* (Table 3; Evans et al., 2005; Evans, 2010).

280 The posterolateral process is missing, exposing part of the narial vestibule in lateral view.
281 In lateral aspect, the posterodorsal process becomes more dorsally inclined posteriorly, in the
282 region representing the anterior part of the base of the crest. As preserved, the posterolateral
283 process suggests a crest-snout angle of ~158° (Table 3), which is closest to the angles mesasured
284 from juvenile *Parasaurolophus* sp. (162°; RAM 14000; Farke et al., 2013), *V. coahuliensis*
285 (157°; CPC-59; Gates et al., 2007), and *H. altispinus* (163°; CMN 2247; Evans, 2010).
286 Additionally the crest-snout angle of the Spring Creek maxilla falls out of the ranges measured

from *Corythosaurus casuarius*: 116–155°, *Hypacrosaurus stebingeri*: 140°–150°, and *Lambeosaurus* sp. 62–156° (Evans et al., 2005; Evans, 2010; Brink et al., 2011, 2014).

Maxilla—The right maxilla (UALVP 59881b) retains the typical triangular body seen in all hadrosaurids (Horner et al., 2004; Evans, 2010; Brink et al., 2011), despite lacking most of the dorsal process and roughly half of the maxillary body anterior to the dorsal process (Fig. 6A). The anterior fracture represents a dorsoventral shear revealing a cross-section of the most anteriorly preserved maxillary tooth family, showing at least three replacement teeth enclosed within the maxillary body (Fig. 6E). In dorsal view (Fig. 6C, D, and E), a shelf that would have supported the posterolateral process of the premaxilla extends medially from the maxillary body (Horner et al., 2004). Lateral to the medial shelf is a large dorsal foramen that opens along the anterodorsal margin of the dorsal process (Fig. 6C); the presence of a foramen at this location is characteristic of lambeosaurines (Horner et al., 2004). Lateral to the large dorsal foramen is a smaller foramen (Fig. 6C), as also seen in juvenile *C. casuarius* (ROM 759: Evans et al., 2005).

In the lateral aspect, the preserved portion of the dorsal process extends dorsally, forming an angle of ~151° with the anterodorsal edge of the maxillary body (Fig. 6A; Table 3). This angle is similar to that seen in juvenile *C. casuarius* (e.g., ROM 759) and *L. lambei* (e.g., ROM 758), as well as *V. coahuilensis* (Gates et al., 2007), but differs from the more obtuse angles seen in subadult *H. stebingeri* (TMP 1994.385.0001: Brink et al., 2011), juvenile *H. altispinus* (CMN 2247: Evans, 2010), and juvenile *Parasaurolophus* (RAM 14000: Farke et al., 2013). The lateral aspect of the dorsal process is mostly occupied by the sutural surface for the jugal, which is anteriorly delimited by a distinct, roughly arcuate ridge. The shape of the ridge indicates that the anterior process of the jugal was broadly rounded, as in most lambeosaurines (Lull & Wright, 1942; Evans et al., 2005; Evans, 2010; Brink et al., 2011), rather than distinctly pointed as

typically observed in hadrosaurines and *Parasaurolophus* (Horner, 1983, 1992; Prieto-Márquez & Norrell, 2010; Bell, 2011a; Prieto-Márquez, 2012; Xing et al., 2017).

The ectopterygoid ridge projects from the maxilla laterally at a level ventral to the contact surface for the jugal and extends anteroposteriorly along the posterior two-thirds of the preserved maxillary body. In the lateral aspect, the ridge is mostly parallel to the tooth row but is deflected ventrally at the posterior end. In dorsal view and posterior to the dorsal process, the ectopterygoid ridge forms a mediolaterally broad shelf. Viewed posteriorly, the lateral margin of the shelf forms a lip curving ventrally similar to *Parasaurolophus* sp. (RAM 14000: Farke et al., 2013), *M. laticaudus* (Prieto-Márquez et al., 2012) and *H. altispinus* (CMN 8675: Evans, 2010). The ectopterygoid ridge partially covers the posteriormost foramen of a series of three foramina piercing the lateral surface of the maxillary body. Although these foramina consistently occur in the same general area in lambeosaurines, the specific number, shape, and position of these foramina are subject to individual and ontogenetic variation (Evans, 2010).

The nearly horizontal maxillary tooth row extends anteroposteriorly along the entire preserved length of the maxilla. The incomplete tooth row includes 23 identifiable tooth families, which alternate between one or two functional teeth on the occlusal surface (Fig. 6F). The number of functional teeth per tooth family ranges from one to three in hadrosaurids (Horner et al., 2004).

Postorbital—The nearly complete left postorbital (UALVP 59902) is triradiate in lateral view, typical for hadrosaurids (Lull & Wright, 1942). Three major processes are preserved; the anterior process, anteroventrally oriented jugal process, and posteriorly oriented squamosal process. A smaller medial process is also preserved (Fig. 7). The postorbital has undergone evident diagenetic distortion, the dorsal and lateral surfaces having been flattened into one plane.

In connection with this, there is a large depression on the dorsal surface of the anterior process and a corresponding sinuous crack on the ventral surface, although such a crack may represent a groove for nerves and blood vessels.

The anterior process is broad mediolaterally and triangular, with a deeply interdigitated sutural surface for the prefrontal along its anteromedial margin. There are no signs of doming at the prefrontal sutural surface (Table 3), unlike *Kazaklambia convincens*, where a prominent postorbital dome occurs on the dorsal surface of the bone (Bell and Brink, 2013). The prefrontal sutural surface terminates posteriorly at a small medial process, marking the separation between the prefrontal and the frontal sutural surfaces. Accordingly, the frontal was excluded from the orbital margin, as is typical for lambeosaurines (Horner et al., 2004). The medial process is dorsoventrally broad at its base and tapers medially, suggesting that it underlay the prefrontal and frontal contact and was thus not visible in dorsal view. Posterior to the medial process, the sutural surface for the frontal is less interdigitated than that for the prefrontal and bears a longitudinally oriented groove that opens dorsomedially. In dorsal view, the frontal sutural surface is distinctly concave, owing to the aforementioned medial process combined with a more posteriorly positioned one that would have extended medially to contact the parietal (Horner, 1992; Evans et al., 2005; Evans, 2010). The ventral margin of the anterior process of the postorbital and the anterior margin of the jugal process form the posterodorsal rim of the orbit. The orbital rim is slightly rugose and is not pierced by a foramen, present in *Amurosaurus riabinini*, *Prosaurolophus maximus*, and *Maiasaura peeblesorum* (Horner, 1983, 1992; Godefroit et al., 2004).

The jugal process is damaged at its midpoint, resulting in an unnatural anterior deflection of the ventral end. The lateral surface of the jugal process is concave, as seen in the juvenile *C.*

356 *casuarius* (AMNH 5461), and is broader anteroposteriorly than that of *Parasaurolophus*, though
357 not to the extent seen in *Edmontosaurus* (Parks, 1922; Wiman, 1931; Ostrom, 1961, 1963;
358 Campione & Evans, 2011). The medial surface of the jugal process bears a prominent
359 dorsoventral ridge that bifurcates dorsomedially to form a V-shaped fossa for the dorsolateral
360 process of the laterosphenoid. This fossa is typically hemispherical/semicircular in hadrosaurids
361 [e.g., *Prosaurolophus maximus* (MOR 447 6.24.6.2), *E. regalis* (ROM 53513 and 53514),
362 *Brachylophosaurus canadensis* (MOR 1071 6.30.89.4), and *L. magnicristatus* (Evans and Reisz,
363 2007).

364 The squamosal process is the longest of the main postorbital processes. The ventral
365 margin of the process, which forms the dorsal rim of the infratemporal fenestra, is arcuate (Table
366 3), similar to that seen in juvenile *H. stebingeri* (TMP 1994.385.01; Brink et al., 2011) and *C.*
367 *casuarius* (ROM 759; Evans et al., 2005), but unlike the straight margins seen in juvenile
368 *Parasaurolophus* sp. (RAM 14000; Farke et al., 2013), *K. convincens* (PIN 2230/1; Bell and
369 Brink 2013), and *Lambeosaurus* sp. (ROM 758; Brink et al., 2011). The squamosal process is
370 also unlike the autapomorphic "dorsally positioned, high arching squamosal process" seen in *V.*
371 *coahuilensis* (CPC-59; Gates et al., 2007). The posterior end of the process is lateromedially
372 expanded, as in other lambeosaurines (Lull & Wright, 1942; Farke et al., 2013), and bifurcated,
373 as in all lambeosaurines except *H. altispinus* (Evans, 2010). The ventromedial surface of the
374 squamosal process bears an anteroposteriorly oriented groove, and the area lateral to the groove
375 is broader and more prominent than that medial to the groove.

376

377 Histology

A general pattern of bone microstructure is present across the eight sampled humeri. The humeri comprise a thick layer of cortical bone externally, and a core of trabecular bone positioned at the centre of the diaphysis. No humeri exhibit a hollow medullary cavity. The trabeculae consist of parallel-fibred bone, although the deepest part of the core of trabecular bone is destroyed in most specimens due to diagenetic modification. External to the inner cancellous bone, most sections show regions of dense Haversian systems that have replaced the primary bone matrix (Fig. 8).

The outer half of the cortex comprises woven-fibred bone that ranges from plexiform to reticulate, transitioning to laminar bone towards the periosteal surface. Open osteonal canals are sporadically present on the periosteal surfaces of the humeri; we identified no external fundamental systems. Resorption fronts are present in all sections. Regions of Haversian reconstruction are restricted to the innermost layers and do not appear within the outer laminar layer. Neither annuli nor lines of arrested growth (LAGs) were observed in any of the sections. All aspects of bone microstructure indicate that skeletal growth was incomplete at the time of death.

Taphonomy

Assemblage data—A total of N=351 vertebrate specimens were collected from the SCBB, including partial and complete teeth, ossified tendons, and bones. The NISP is 273, of which NPSP=142. Almost all (99.7%) of the identifiable specimens are assigned to Hadrosauridae, with only a single tyrannosaurid tooth as direct evidence of a second taxon within the bonebed, although toothmarks suggest other taxa were present before deposition. The

three cranial elements described above can be referred to Lambeosaurinae. Based on the number of right humeri collected (Fig. 4, Table 1), the current MNI of hadrosaurids is eight.

The maximum preserved lengths of individual specimens range from 10–640 mm (mean = 166 mm; median = 136 mm). Specimen lengths are positively skewed (skewness = 1.4918), the vast majority of elements being <400 mm in total length. Complete examples of each type of element tend to be uniform in size, indicating the occurrence of a single growth stage, which is supported by the histological results. Complete femora range from 558 mm to 640 mm, placing them in the late juvenile growth stage (sensu Horner et al. 2000). Total lengths of postcranial elements, scaled against a complete *Lambeosaurus* sp. (AMNH 5340) skeleton (Farke et al., 2013), suggest a total body length estimate of ≤4.3 m (Table 4).

The vast majority of the bones were found disarticulated, with limited signs of association. The only possible exception pertains to a dentary, a predentary, and a mass of articulated teeth that were all found within an area < 0.5 m^2 (Fig. 2). The representation of Voorhies groups in the SCBB sample is more uniform than expected, given the juvenile hadrosaurid skeleton structure (Table 2; $X^2 = 41.746$, p-value <<0.001). In particular, there is a significant underrepresentation of Voorhies group I relative to groups II and III.

Quarry Data—The lateral extent of the 2018 and 2019 excavations was approximately 18 m, and the total excavation area was 35 m^2 (Fig. 2). A femur recovered ~15 m upstream from the main excavation site, of similar size and preservation style to those recovered from the quarry, suggests a possible lateral extent of up to 33 m for the SCBB. The fossiliferous horizon is limited to the bottom 40 cm of a ~2 m thick mudstone layer with no distinct grading of bioclasts. Crevices (10–15 cm wide) found within the quarry walls suggest widespread slumping and the possible displacement of the entire bonebed from its original position. The density of bones

within each grid square ranges from 1 to 30 bones/m^2, with a mean of 7.5 bones/m^2. Preferential alignment of long bones was difficult to determine from the SCBB as Rao's spacing test suggests a significant departure from uniformity (test statistic = 183.6; critical value (at p = 0.05) = 143.8), whilst Kuiper's test of uniformity suggests a uniform distribution (test statistic = 1.05; critical value (at p = 0.05) = 1.7). This inconsistency between tests may be related to the high circular variance ($\sigma^2 = 0.93$) caused by high bone orientation variability (Fig. 2). Patchiness indices >1 were recorded from both 2018 and 2019 excavations (1.67 and 1.35, respectively), suggesting clumping of specimens rather than a random distribution.

Bone Modification—Of the prepared specimens from the SCBB, 44.2% are complete (Table 5), ranging in size from small cranial elements to relatively large hindlimb elements. A mixture of transverse post-burial fractures and perimortem spiral fractures represents the most common fracture style, observed on 38.9% of the NPSP. Signs of abrasion are rare within the SCBB, with only 13.9% of the NPSP showing low-level abrasion (stages 0 and 1) and <2% exhibiting more severe levels (stages 2 and 3). Similarly, 89.7% of NPSP show little to no weathering (weathering stages 0–1; Table 5, Fig. 4). The remaining 10.3% were observed to be at weathering stage 2.

Biogenic modification of some bones in the sample can be inferred based on the presence of parallel striae, which result from bone–substrate interactions and imply trampling (Behrensmeyer et al., 1986). Approximately 33% of the prepared specimens exhibit such striae. The aforementioned perimortem spiral fractures are also consistent with trampling. Tooth marks are present on 3.8% of NPSP and are represented by pits and conspicuous parallel score marks; these marks primarily occur on limb bones. Given that the tooth marks are predominantly small, U-shaped furrows (Fig. 9), it is likely that they were produced by small scavengers, potentially

446 including small theropods (Bell & Campione, 2014; Bell & Currie, 2015). Some scavenging by
447 larger theropods may have occurred based on the presence of a single shed tyrannosaurid tooth
448 and toothmarks potentially left by smaller tyrannosaurid individuals. Finally, only a single
449 notable pathology is present on the supra-acetabular process of an incomplete ilium (UALVP
450 60540, Fig. 9). The pathology comprises a hemispherical erosion of the lateral surface of the
451 process, with smooth margins but an irregular and rugose internal surface.

452

453 Discussion

454 Systematics of the Spring Creek hadrosaurids

455 The Spring Creek hadrosaurids were preliminarily assigned to the hadrosaurid clade
456 Hadrosaurinae (or Saurolophinae, sensu Prieto-Márquez, 2010) based on the low deltopectoral
457 crests observed on the humeri (Tanke, 2004). However, the prominence of the crest is known to
458 vary ontogenetically, especially among lambeosaurines (Egi & Weishampel, 2002; Horner et al.,
459 2004), rendering this assignment questionable. The skull elements described in this study
460 represent the first diagnostic cranial material from the SCBB and unequivocally support a
461 lambeosaurine designation based on the following synapomorphies: external naris fully enclosed
462 by the premaxilla, large oblate foramen opening dorsally on the anterodorsal margin of the
463 maxilla, and jugal sutural surface on the maxilla with a broadly rounded anterior margin (Evans,
464 2010; Prieto-Márquez, 2010). Furthermore, the postorbital would have contacted the prefrontal,
465 excluding the frontal from the orbital margin. This condition is typical of lambeosaurines,
466 despite being present in the hadrosaurines *Prosaurolophus* and *Saurolophus* (Horner, 1992;
467 Horner et al., 2004; Bell, 2011a, 2011b; McGarrity et al., 2013). The other specimens so far

468 recovered from the SCBB are not diagnostic below Hadrosauridae. However, given their
469 consistent size and the absence of conspicuous variations that could indicate the presence of
470 multiple taxa, it is likely that all hadrosaurid specimens from the SCBB pertain to the same
471 species.

472 Unfortunately, the available sample of disarticulated juvenile elements provides limited
473 diagnostic information, making any taxonomic designation below Lambeosaurinae ambiguous.
474 The relatively acute angle between the body and dorsal process of the maxilla (Fig. 6) is more
475 consistent with that seen in *C. casuarius* and *Lambeosaurus* (Lull & Wright, 1942; Evans et al.,
476 2005) than that seen in *Hypacrosaurus* and *Parasaurolophus* (Evans, 2010; Brink et al., 2011;
477 Farke et al., 2013). Similarly, the arched profile of the postorbital squamosal process is akin to
478 that in *C. casuarius* and *L. magnicristatus* (Evans & Reisz, 2007). By contrast, the more
479 anteriorly attenuated bony naris of the premaxilla (Fig. 5) resembles that of *H. altispinus* and
480 *Lambeosaurus* (Lull & Wright, 1942; Ostrom, 1961; Evans et al., 2005; Gates et al., 2007;
481 Evans, 2010; Brink et al., 2011), and the relatively obtuse snout–crest angle of the premaxilla is
482 most consistent with *H. altispinus* (Evans, 2010; Brink et al., 2014); but note that the postorbital
483 squamosal process (UALVP 59902; Fig. 7) differs from that of *H. altispinus* in being bifurcated
484 (Evans, 2010).

485 The SCBB lies within the upper strata of Unit 3 of the Wapiti Formation, which is
486 roughly contemporaneous with the Bearpaw Formation and the Drumheller and Strathmore
487 members of the lower Horseshoe Canyon Formation (Fig. 10). The SCBB lambeosaurines are,
488 therefore, younger than known species of *Corythosaurus*, *Lambeosaurus*, and *Parasaurolophus*
489 from the Dinosaur Park Formation and intermediate in age between *H. stebingeri* and *H.*
490 *altispinus* from the Two Medicine and Horseshoe Canyon formations, respectively (Horner &

Currie, 1994; Brink et al., 2011; Mallon et al., 2012; Eberth & Kamo, 2020). As a result, the SCBB is apparently not contemporaneous with any other hadrosaurid species known from Canada or the U.S.A. (Fig. 10), although it may be contemporaneous with the Mexican lambeosaurines *V. coahuilensis* (Cerro del Pueblo Formation; Gates et al., 2007) and *M. laticaudatus* (El Gallo Formation; Prieto-Márquez et al., 2012).

The SCBB is geographically located between the northernmost lambeosaurine in Alaska (Takasaki et al., 2019) and those from southern Alberta (Fig. 10). Moreover, the SCBB is at a far higher paleolatitude than the contemporaneous Mexican lambeosaurine localities (Fig. 10). Faunal endemism was suggested for at least Unit 3 of the Wapiti Formation based on the occurrence of *P. lakustai* and *B. certekorum*, both of which are uniquely known from the Pipestone Creek Bonebed (Currie et al., 2008b; Bell & Currie, 2016), although such endemism may be stratigraphic rather than biogeographic (Fowler, 2017). Additionally, the occurrence of *E. regalis* in Unit 4 may reflect a shift from endemism to dinosaur cosmopolitanism across Alberta (Bell et al., 2014a).

The fact that the SCBB specimens are geographically and/or stratigraphically isolated from all other documented lambeosaurine occurrences, combined with the potential rapid evolutionary turnover of lambeosaurines, as evinced from the Dinosaur Park Formation (Mallon et al., 2012), and the conflicting morphological signals described above, suggests that the lambeosaurine material from the SCBB may well represent a new species unique to the Wapiti Formation. Unfortunately, such a conclusion cannot be considered secure in the absence of more complete, especially more mature, cranial material that reveals a unique suite of character states. Irrespective of its precise taxonomic identification, the SCBB sample represents the first lambeosaurine material reported from the Wapiti Formation. The presence of a lambeosaurine in

514 Unit 3 supports a similarity in overall faunal composition between portions of the Wapiti
515 Formation in northwestern Alberta to those from the southeast (Fanti & Catuneanu, 2009;
516 Mallon et al., 2012; Eberth et al., 2013; Fanti et al., 2013; Fowler, 2017; Eberth & Kamo, 2020).
517 Furthermore, this discovery supports the hypothesis that Late Cretaceous lambeosaurine
518 distributions extend into high-latitude regions, recently suggested based on an isolated
519 supraoccipital from the Prince Creek Formation of Alaska (Takasaki et al., 2019).

520

521 Taphonomy of the Spring Creek Bonebed

522 The SCBB is essentially monospecific, containing the remains of at least eight juvenile
523 lambeosaurines (thus far represented by 350 hadrosaurid bones) and one tyrannosaurid
524 (represented by a single shed tooth), which are inferred to have been buried in an organic-rich,
525 quiet-water setting based on the bonebeds mud-hosted facies. The tyrannosaurid tooth likely
526 entered the assemblage via scavenging rather than through the same event that caused the death
527 of the lambeosaurines, as non-dental tyrannosaurid material is yet to be recovered from the
528 bonebed. Furthermore, the light to minimal weathering (Table 5; Fig. 4) indicates that all the
529 bones remained exposed for about the same length of time [<12 months; as identified by
530 Behrensmeyer (1978) and Fiorillo (1988)] Together, these observations suggest that the juvenile
531 lambeosaurines perished in a mass mortality event, rather than through gradual attrition (Bell &
532 Campione, 2014; Chiba et al., 2015; Funston et al., 2016; Ullmann et al., 2017).

533 The killing mechanism for the SCBB lambeosaurines remains unknown. The
534 pathological lesion observed on a partial ilium (UALVP 60540; Fig. 9) resembles features
535 resulting from Langerhans Cell Histiocytosis inferred in other hadrosaurids, based on its smooth

margin and "wrinkled" internal surface (Rothschild et al., 2020). However, it is intuitively implausible that an osteologically borne disease instigated the mass mortality event. Coastal-plain flooding has been interpreted as the typical source of macrofossil bonebeds throughout the Upper Cretaceous of Alberta (Eberth, 2015). Like those hosting the SCBB, floodplain deposits are common within Unit 3 of the Wapiti Formation, attesting to periodic inundation while the formation was being deposited (Fanti & Catuneanu, 2009). However, the absence of aquatic vertebrates and the lack of either advanced hydraulic reworking or channel sediments indicate that the SCBB lambeosaurines did not drown within a channel (Bell & Campione, 2014). Additionally, the laminar bone deposited near the periosteal surface of sectioned humeri may indicate slower bone growth, suggesting that the SCBB lambeosaurines died during a cold or dry season (Wosik et al., 2020).

Following the mass mortality event, the lambeosaurine cadavers were exposed long enough for scavenging, trampling, and disarticulation to occur but were buried before substantial weathering could take effect. The ubiquitous disarticulation in the SCBB is most likely a product of skeletal immaturity, which sees juveniles disarticulating more rapidly than adults (Hill & Behrensmeyer, 1984; Horner & Currie, 1994). Scavenging and trampling, inferred from the presence of tooth marks, parallel striae, and spiral fractures, may have also contributed to disarticulation. However, scavenging processes were likely minor given the low occurrence of bite-marks (3.8%; Table 5) compared to other sites, such as the Danek Bonebed (30%; Bell & Campione, 2014), Bleriot Ferry Bonebed (~10%; Evans et al., 2015), and Scabby Butte Bonebed: Site 2 (6.2%; Campbell et al., 2019).

A significantly higher incidence of bones within Voorhies groups II and III at the SCBB (χ^2=41.746, *P*-value << 0.001; Table 2) indicates the selective removal of some smaller, more

559 transportable elements. Presumably, fluvial factors were the primary sorting mechanism
560 (Voorhies, 1969), although some small elements, including haemal arches and metacarpals, were
561 preserved. Tooth marks and parallel striae suggest that scavenging and trampling, respectively,
562 occurred at the SCBB but, given their low incidence, likely represented minor sorting roles
563 compared to fluvial influences. The preservation of hadrosaurid teeth articulated within a dentary
564 (UALVP 59900) is significant because the fragile lingual sheet of bone that keeps the teeth
565 within the dentary is highly susceptible to post-mortem damage, indicating that the SCBB
566 lambeosaurines were buried before such early deterioration could occur (Bell & Campione,
567 2014). Moreover, the scarcity of teeth within hadrosaurid bonebeds has been used to support a
568 'bloat-and-float' scenario (Gangloff & Fiorillo, 2010), during which teeth are lost as a result of
569 hydraulic transport, following the loss of the thin lingual sheet. The presence of articulated and
570 isolated teeth in the SCBB is inconsistent with this scenario and suggests little to no transport
571 from the site of death. Although Rao's spacing test suggested a significant NE–SW preferred
572 orientation, the substantial circular variance around this modal orientation (Fig. 2) suggests a
573 generally low fluvial influence on long bone alignment. Additionally, high patchiness indices
574 and some skeletal associations suggest little reworking/transport of elements. Overall lack of
575 abrasion in the sample (Table 5) also suggests limited transport (Hunt, 1978; Fiorillo, 1988),
576 although the relationship between abrasion and transport can be highly variable (Behrensmeyer,
577 1982; Argast et al., 1987; Eaton et al., 1989). Given the above taphonomic evidence, we cannot
578 unambiguously reject that some transport of elements occurred, and thus the SCBB can be
579 conservatively regarded as a parautochthonous mass mortality bonebed.

580

581 Growth dynamics of the SCBB lambeosaurines

582 Based on their observed bone microstructure, the SCBB lambeosaurines were undergoing
583 sustained, but not rapid, growth at their time of death (Horner & Currie, 1994; Horner et al.,
584 2000; Hubner, 2012). The regions of reticular to plexiform bone preserved in the deeper parts of
585 the outer cortex indicate recent periods of rapid growth, whereas the presence of secondary
586 osteons coupled with the increased organization of the laminar bone towards the periosteal
587 surface suggest that individuals were experiencing a slower growth rate (Horner et al., 1999;
588 Horner et al., 2000; Huttenlocker et al., 2013). Scaling of limb bones from the SCBB to those of
589 an articulated juvenile *Lambeosaurus* indicates that the individuals had attained a total body
590 length of ≤ 4.2 m (Table 4; *Lambeosaurus* data from Farke et al., 2013), which is around half the
591 7–10 m total body length observed in most adult hadrosaurids or a third of the total ~12 m length
592 reached by giant hadrosaurids (Prieto-Márquez et al., 2012; Hone et al., 2014).

593 Attempts to infer hadrosaurid growth strategies from histological analyses are
594 inescapably convoluted, to say the least. In *Maiasaura peeblesorum*, Horner et al. (2000)
595 identified six distinct ontogenetic stages based on bone microstructure patterns and the total
596 lengths of associated femora: early and late nestling, early and late juvenile, sub-adult, and adult.
597 The SCBB lambeosaurines bear the greatest histological resemblance to the late juvenile stage,
598 as sectioned humeri display: 1) laminar, plexiform, and reticular bone, 2) Haversian
599 reconstruction, including secondary osteons, 3) spongiose, but not hollow, marrow cavities, and
600 4) no evidence of LAGs or an external fundamental system (Horner et al., 2000). Late juveniles
601 are hypothesized to exhibit moderate to high growth rates and, based on bone diametral
602 increases, should have reached the late juvenile stage 1.1–2.4 years after hatching (Horner et al.,
603 2000, Wosik et al., 2020). However, the SCBB lambeosaurines possibly had a different
604 ontogenetic trajectory to that described for *Maiasaura*.

The lack of LAGs among the sampled SCBB humeri is consistent with a late juvenile designation. In *M. peeblesorum*, 0–1 LAGs were indicative of a late juvenile growth stage (Horner et al., 2000). Vanderven et al. (2014) demonstrated that, in *E. regalis*, LAGs occur more frequently in humeri than in femora of *E. regalis*, a pattern thought to reflect slower humeral growth. A single LAG was observed in the smallest *E. regalis* humerus, although this specimen was ~140 mm longer than the humeri collected from the SCBB. LAGs were previously interpreted as representing annual interruptions in growth (Horner et al., 1999; Horner et al., 2000; Chinsamy et al., 2012; Vanderven et al., 2014; Woodward et al., 2015), and it is, therefore, possible that the lack of LAGs in the SCBB lambeosaurines means that they were not yet a year old at the time of death, however; given their considerable size, this is unlikely. Alternatively, the lack of LAGs among the sampled SCBB humeri may be environmental rather than ontogenetic (Chinsamy et al., 2012; Vanderven et al., 2014). The Wapiti Formation represents a geographic transition between Alaska's polar faunas and the more temperate zones of southern Alberta and northern Montana (Bell et al., 2014b). As such, the development of bone textural switches in *Edmontosaurus* sp. from Alaska could be the result of polar overwintering, with harsher seasons leading to growth interruption (Chinsamy et al., 2012), although distinct LAGs have also been noted in some hadrosaurids from temperate latitudes (Horner et al., 1999). Nevertheless, the lack of LAGs at the SCBB may suggest that Unit 3 of the Wapiti Formation was deposited under relatively equable climatic conditions (Fanti & Miyashita, 2009). In any case, the use of LAGs to determine absolute age is evidently ambiguous, especially for humeri (Horner et al., 2000; Erickson et al., 2001; Vanderven et al., 2014; Woodward et al., 2015). We, therefore, adopt the more conservative approach of assigning the SCBB lambeosaurines to the

late juvenile stage based on their degree of histological similarity with late juvenile individuals of *M. peeblesorum* (Horner et al., 2000), and their overall body size.

Age segregation in hadrosaurids

Taphonomic data and the lack of adult or perinatal material indicate that the SCBB lambeosaurine material is best interpreted as the remains of a group of late juvenile individuals that perished in a single mass mortality event. Accordingly, the composition of the SCBB may reflect a demographic phenomenon known as age segregation—the aggregation and segregation of individuals of the same species based on age, typically in response to resource or spatial limitations (Rogers & Kidwell, 2007; Pelletier et al., 2016). Among dinosaurs, age segregation has been proposed as an explanation for juvenile-dominated bonebed samples of sauropods (Myers & Fiorillo, 2009), theropods (Raath, 1990; Currie, 1998; Zanno & Erickson, 2006; Varricchio et al., 2008), ceratopsians (Gilmore, 1917; Lehman, 2006; Mathews et al., 2007; Zhao et al., 2014), thyreophorans (Galton, 1982; Jerzykiewicz et al., 1993; McWhinney et al., 2004), and ornithopods, including lambeosaurines (Dodson, 1971; Norman, 1987; Forster, 1990; Varricchio & Horner, 1993; Scherzer & Varricchio, 2010; Eberth, 2015; Vila et al., 2016; Wosik et al., 2020). Food is a limited resource in most ecosystems, and sympatric species often employ interspecific niche partitioning strategies to minimize the adverse effects of competition (Farlow, 1976; du Toit & Cumming, 1999; Lehman, 2001; Mallon & Anderson, 2014). However, ecomorphological data have only distinguished major dinosaurian clades (e.g., ceratopsians vs. hadrosaurids vs. ankylosaurs), and it remains unclear how, and indeed whether, closely related species may have mitigated the effects of mutual competition (Mallon & Anderson, 2014). It is, therefore, possible that in dinosaurs, such as hadrosaurids, such mitigation was achieved via

intra- rather than interspecific dynamics, with juveniles and adults partitioning food based on either dietary requirements and/or physiological capabilities. For instance, the fitness costs of dietary synchronization in sauropods (such as those associated with movement to new foraging areas and the need for more resting time) as a result of size difference between juveniles and adults were possibly eased by age segregation and age-based niche partitioning, a scenario supported by the existence of ontogenetically variable dental microwear patterns (Fiorillo, 1998; Myers & Fiorillo, 2009; Zhao et al., 2014; Pelletier et al., 2016). To date, the possibility of similar ontogenetic variation in dental microwear has not been investigated in hadrosaurids. However, younger hadrosaurids were clearly unable to reach the same maximum feeding heights as adults, implying that juveniles must have had a more restricted feeding envelope unless they were actively fed by mature individuals. Accordingly, the SCBB and other age-segregated bonebeds (Varricchio et al., 2008; Myers & Fiorillo, 2009; Scherzer & Varricchio, 2010; Eberth & Braman, 2012) may be a product of population-level resource partitioning strategies that mitigated competition between diverse communities of megaherbivorous dinosaurs (Mallon et al., 2012; Mallon & Anderson, 2013; Mallon et al., 2013; Mallon & Anderson, 2014).

An alternate explanation for age segregation at the SCBB, though one not mutually exclusive with resource partitioning, is that hadrosaurid life history and breeding strategies led to seasonal variation in the age structure among a population (Varricchio, 2011; Zhao et al., 2014). Aggregations of hadrosaurid nesting sites indicate colonial nesting behaviours in both lowland and upland areas (Horner, 1982; Tanke & Brett-Surman, 2001; Fanti & Miyashita, 2009). During nesting times, non-breeding individuals may have segregated away from the breeding population, being relatively large (~50% of typical adult size; Table 4), but potentially still sexually immature (Varricchio et al., 2008; Varricchio, 2011, Wosik et al., 2020). However, such

673 segregated groups are liable to contain a spectrum of ages (e.g., early–late juveniles; Varricchio
674 et al., 2008; Zhao et al., 2014), which is not the case for the SCBB lambeosaurines. Finally, age
675 segregation could be the result of annually cyclical parental caring behaviours, in which young
676 were reared for an extended period within a yearly cycle, as observed in most modern
677 crocodilian and avian species (Thorbjarnarson & Hernandez, 1993; Davies, 2002). Such parental
678 caring behaviours have been inferred from multiple dinosaur bonebeds, including those of
679 hadrosaurids (Horner & Makela, 1979), and supported by egg-adult associations (Varricchio,
680 2011).

681 Dinosaurs exhibited complex life histories and behavioural flexibility (e.g. Myers &
682 Fiorillo, 2009; Varricchio, 2011), and there is still much about their palaeoecology that we do not
683 understand (Mallon & Anderson, 2013; Mallon et al., 2013; Mallon & Anderson, 2014).
684 Moreover, as we cannot readily distinguish between males and females in the dinosaur fossil
685 record, we cannot reject the possibility that age-segregated dinosaur bonebeds were sexually
686 segregated as well (Myers & Fiorillo, 2009; Pelletier et al., 2016), as was implied by Tanke
687 (2004) in his original report, referring to the assemblage as a ‘bachelor herd’. Regardless of
688 whether sex-segregation was typical of juvenile hadrosaurid bonebeds, such deposits offer a
689 wealth of insights into growth and social behaviour in these ubiquitous herbivores and will
690 undoubtedly reward further research.

691

692 ## Conclusion

693 This study marks the first formal description of the Spring Creek Bonebed and the first
694 definitive documentation of lambeosaurines from the Wapiti Formation, here preserved within

Unit 3. A total of 351 specimens were thus far collected from the bonebed, from which we identified a minimum of eight juvenile individuals based on non-overlapping humeri. Interestingly, unique spatiotemporal and conflicting morphological signatures hint at the presence of a new lambeosaurine species within the formation. However, given their ontogenetic state and the difficulties associated with identifying even complete juvenile specimens to a genus or species (Evans et al., 2005; Brink et al., 2014), we feel that a conservative indeterminate Lambeosaurinae designation is the most appropriate at this time.

The seemingly exclusive preservation of a single age class adds to our understanding of dinosaurian life histories, further supporting that breeding, seasonality, and/or dietary partitioning may contribute to dinosaur demographics. Future research into macrofossil bonebeds, particularly from the Wapiti Formation, will undoubtedly provide a greater understanding of dinosaur diversity, distribution, and life history strategies during the final stages of the Mesozoic.

Acknowledgements

This study was completed as part of BH's Master of Science degree at the University of New England, Australia, supervised by NEC and PRB. Thanks are given to John Scannella and Amy Atwater (Museum of the Rockies), Kevin Seymour (Royal Ontario Museum), Brandon Strilisky and Rebecca Sanchez (Royal Tyrell Museum of Paleontology), and Cam Reed and Calla Scott (Philip J. Currie Dinosaur Museum) for access to and help with their respective collections. Special thanks to Malcolm Lambert for preparing histological samples of TMP specimens and to Russell Bicknell (University of New England) for capturing of images for supplementary figure

2C and D. We are grateful to Grande Prairie Regional College, who facilitated fieldwork in the Peace Region of northwestern Alberta, and to the many volunteers during the 2018 and 2019 BADP expeditions. This research was funded by a Research Training Program and Rural and Regional Enterprise scholarships to BH, a Dinosaur Research Institute (DRI) Student Project Grant to BH, a DRI Dinosaur Fieldwork in Western Canada to NEC and MJV, an Australian Research Council Discovery Early Career Research Award to NEC (DE190101423), and a Natural Sciences and Engineering Research Council Discovery Grant (RGPIN-2017-06246) and an endowment associated with the Philip J. Currie Professorship at the University of Alberta to CS. The authors would also like to thank the editor and reviewers for their comments and help getting this study over the line.

References

Argast, S., Farlow, J. O., Gabet, R. M., & Brinkman, D. L. (1987). Transport-induced abrasion of fossil reptilian teeth: implications for the existence of Tertiary dinosaurs in the Hell Creek Formation, Montana. *Geology, 15*(10), 927-930.

Badgley, C. (1986). Taphonomy of Mammalian Fossil Remains from Siwalik Rocks of Pakistan. *Palaeobiology, 12*(2), 119-142.

Behrensmeyer, A. K. (1978). Taphonomic and ecologic information from bone weathering. *Paleobiology, 4*(2), 150-162.

Behrensmeyer, A. K. (1982). Time Resolution in Fluvial Vertebrate Assemblages. *Paleobiology, 8*(3), 211-227.

738 Behrensmeyer, A. K. (1991). Terrestrial Vertebrate Accumulations. In P. A. Allison & D. E. G. Briggs (Eds.),
739 *Taphonomy: Releasing the Data Locked in the Fossil Record* (Vol. 9, pp. 291-335). New York:
740 Plenum Press.
741 Behrensmeyer, A. K., Gordon, A. K., & Yanagi, K. D. (1986). Trampling as a cause of bone surface damage
742 and pseudo-cutmarks. *Nature, 319*(6056), 768-771.
743 Bell, P. R. (2011a). Cranial Osteology and Ontogeny of *Saurolophus angustirostris* from the Late
744 Cretaceous of Mongolia with Comments on *Saurolophus osborni* from Canada. *Acta*
745 *Palaeontologica Polonica, 56*(4), 703-722. doi:10.4202/app.2010.0061
746 Bell, P. R. (2011b). Redescription of the skull of *Saurolophus osborni* Brown 1912 (Ornithischia:
747 Hadrosauridae). *Cretaceous Research, 32*(1), 30-44. doi:10.1016/j.cretres.2010.10.002
748 Bell P. R., Brink K. S. (2013). Kazaklambia convincens comb. nov., a primitive juvenile lambeosaurine
749 from the Santonian of Kazakhstan. Cretaceous Research. 45:265-274.
750 Bell, P. R., & Campione, N. E. (2014). Taphonomy of the Danek Bonebed: a monodominant
751 *Edmontosaurus* (Hadrosauridae) bonebed from the Horseshoe Canyon Formation, Alberta.
752 *Canadian Journal of Earth Sciences, 51*(11). doi:10.1139/cjes-2014-0062
753 Bell, P. R., & Currie, P. J. (2016). A high-latitude dromaeosaurid, *Boreonykus certekorum*, gen. et sp. nov.
754 (Theropoda), from the upper Campanian Wapiti Formation, west-central Alberta. *Journal of*
755 *Vertebrate Paleontology, 36*(1). doi:10.1080/02724634.2015.1034359
756 Bell, P. R., Fanti, F., Currie, P. J., & Arbour, V. M. (2014a). A Mummified Duck-Billed Dinosaur with a Soft-
757 Tissue Cock's Comb. *Current Biology, 24*(1), 70-75. doi:10.1016/j.cub.2013.11.008
758 Bell, P. R., Fanti, F., & Sissons, R. (2013). A possible pterosaur manus track from the Late Cretaceous of
759 Alberta. *Lethaia, 46*, 274-279.

760 Bell, P. R., Sissons, R., Burns, M. E., Fanti, F., & Currie, P. J. (2014b). New Saurolophine Material from the
761 Upper Campanian–lower Maastrichtian Wapiti Formation, West-Central Alberta. In D. Eberth &
762 D. C. Evans (Eds.), *Hadrosaurs* (pp. 174-190). Bloomington, IN: Indiana University Press.
763 Blob, R. W., & Badgley, C. (2007). Numerical Methods for Bonebed Analysis. In R. R. Rogers, D. A. Eberth,
764 & A. R. Fiorillo (Eds.), *Bonebeds: Genesis, Analysis, and Paleobiological Significance* (pp. 333-
765 396). Chicago and London: The University of Chicago Press.
766 Brink, K. S., Zelenitsky, D. K., Evans, D. C., Therrien, F., & Horner, J. R. (2011). A sub-adult skull of
767 *Hypacrosaurus stebingeri* (Ornithischia: Lambeosaurinae): anatomy and comparison. *Historical*
768 *Biology, 23*(1), 63-72. doi:10.1080/08912963.2010.499169
769 Brink, K. S., D. K. Zelenitsky, D. C. Evans, J. R. Horner, and F. Therrien. 2014. Cranial Morphology and
770 Variation in *Hypacrosaurus stebingeri* (Ornithischia: Hadrosauridae). In D. Eberth & D. C. Evans
771 (Eds.), *Hadrosaurs* (pp. 245–265). Bloomington, IN: Indiana University Press.
772 Britt, B. B., Eberth, D. A., Scheetz, R. D., Greenhalgh, B. W., & Stadtman, K. L. (2009). Taphonomy of
773 debris-flow hosted dinosaur bonebeds at Dalton Wells, Utah (Lower Cretaceous, Cedar
774 Mountain Formation, USA). *Palaeogeography, Palaeoclimatology, Palaeoecology, 280*(1-2), 1-
775 22. doi:10.1016/j.palaeo.2009.06.004
776 Campbell, J. A., Ryan, M. J., & Anderson, J. F. (2019). A taphonomic analysis of a multitaxic bonebed
777 from the St. Mary River Formation (uppermost Campanian to lowermost Maastrichtian) of
778 Alberta, dominated by cf. *Edmontosaurus regalis* (Ornithischia: Hadrosauridae), with significant
779 remains of *Pachyrhinosaurus canadensis* (Ornithischia: Ceratopsidae). *Canadian Journal of Earth*
780 *Sciences, 00*, 1-13.
781 Campione, N. E., & Evans, D. C. (2011). Cranial Growth and Variation in Edmontosaurs (Dinosauria:
782 Hadrosauridae): Implications for Latest Cretaceous Megaherbivore Diversity in North America.
783 *PLoS One, 6*(9), e25186. doi:10.1371/journal.pone.0025186

784 Chiba, K., Ryan, M. J., Braman, D. R., Eberth, D. A., Scott, E. E., Brown, C. M., . . . Evans, D. C. (2015).
785 Taphonomy of a Monodominant *Centrosaurus Apertus* (Dinosauria: Ceratopsia) Bonebed from
786 the Upper Oldman Formation of Southeastern Alberta. *Palaios, 30*(9), 655-667.
787 doi:10.2110/palo.2014.084
788 Chinsamy, A., Thomas, D. B., Tumarkin-Deratzian, A. R., & Fiorillo, A. R. (2012). Hadrosaurs Were
789 Perennial Polar Residents. *The Anatomical Record, 295*(4), 610-614. doi:10.1002/ar.22428
790 Christians, J. P. (1992). *Taphonomy and Sedimentology of the Mason Dinosaur Quarry. Hell Creek*
791 *Formation (Upper Cretaceous), South Dakota.* (MSc). University of Wisconsin,
792 Currie, P. J. (1998). Possible evidence of gregarious behavior in tyrannosaurids. *GAIA, 15*, 217-277.
793 Currie, P. J., Langston Jr, W., & Tanke, D. H. (2008a). A new species of *Pachyrhinosaurus* (Dinosauria,
794 Ceratopsidae) from the Upper Cretaceous of Alberta, Canada. A New Horned Dinosaur from an
795 Upper Cretaceous Bone Bed in Alberta. In P. J. Currie, W. Langston Jr, & D. H. Tanke (Eds.), *A*
796 *New Horned Dinosaur from an Upper Cretaceous Bone Bed in Alberta. Ottawa: National*
797 *Research Council of Canada* (pp. 1-108). Ottawa: NRC Research Press.
798 Currie, P. J., Langston, J. W., & Tanke, D. H. (2008b). *A new species of Pachyrhinosaurus (Dinosauria,*
799 *Ceratopsidae) from the Upper Cretaceous of Alberta, Canada*.
800 Davies, S. J. J. F. (2002). *Ratites and Tinamous*. Oxford: Ofxord University Press.
801 Dodson, P. (1971). Sedimentology and taphonomy of the Oldman formation (Campanian), dinosaur
802 provincial park, Alberta (Canada). *Palaeogeography, Palaeoclimatology, Palaeoecology, 10*(1),
803 21-74.
804 du Toit, J. T., & Cumming, D. H. M. (1999). Functional significance of ungulate diversity in African
805 savannas and the ecological implications of the spread of pastoralism. *Biodiversity &*
806 *Conservation, 8*, 1643-1661.

807 Eaton, J. G., Kirkland, J. I., & Doi, K. (1989). Evidence of Reworked Cretaceous Fossils and their Bearing
808 on the Existence of Tertiary Dinosaurs. *Palaios, 4*, 281-286.
809 Eberth, D. A. (2015). Origins of dinosaur bonebeds in the Cretaceous of Alberta, Canada. *Canadian*
810 *Journal of Earth Sciences, 52*, 655-681. doi:10.1139/cjes-2014-0200
811 Eberth, D. A., & Braman, D. R. (2012). A revised stratigraphy and depositional history for the Horseshoe
812 Canyon Formation (Upper Cretaceous), southern Alberta plains. *Canadian Journal of Earth*
813 *Sciences, 49*(9), 1053–1086.
814 Eberth, D. A., & Currie, P. J. (2010). Stratigraphy, sedimentology, and taphonomy of the Albertosaurus
815 bonebed (upper Horseshoe Canyon Formation; Maastrichtian), southern Alberta, Canada.
816 *Canadian Journal of Earth Sciences, 47*(9), 1119-1144. doi:10.1139/E10-045
817 Eberth, D. A., Evans, D. C., Brinkman, D. B., Therrien, F., Tanke, D. H., & Russell, L. S. (2013). Dinosaur
818 biostratigraphy of the Edmonton Group (Upper Cretaceous), Alberta, Canada: evidence for
819 climate influence. *Canadian Journal of Earth Sciences, 50*, 701-726.
820 Eberth, D. A., & Getty, M. A. (2005). Ceratopsian bonebeds: occurence, origins, and significance. In P. J.
821 Currie & E. B. Koppelhus (Eds.), *Dinosaur Provincial Park: A Spectacular Ancient Ecosystem*
822 *Revealed* (pp. 501-536). Bloomington, Indianapolis: Indiana University press.
823 Eberth, D. A., & Kamo, S. L. (2020). High-precision U–Pb CA–ID–TIMS dating and chronostratigraphy of
824 the dinosaur-rich Horseshoe Canyon Formation (Upper Cretaceous, Campanian–Maastrichtian),
825 Red Deer River valley, Alberta, Canada. *Canadian Journal of Earth Sciences, 00*, 1-18.
826 Eberth, D. A., Rogers, R. R., & Fiorillo, A. R. (2007a). A practical approach to the study of bonebeds. In R.
827 R. Rogers, D. A. Eberth, & A. R. Fiorillo (Eds.), *Bonebeds: genesis, analysis, and paleobiological*
828 *significance* (pp. 256-331). Chicago and London: University of Chicago.
829 Eberth, D. A., Shannon, M., & Noland, B. G. (2007b). A Bonebeds Database: Classification, Biases, and
830 Patterns of Occurence. In R. R. Rogers, D. A. Eberth, & A. R. Fiorillo (Eds.), *Bonebeds: Genesis,*

Analysis, and Palaeobiological Significance (pp. 103-220). Chicago and London: The University of Chicago Press.

Egi, N., & Weishampel, D. B. (2002). Morphometric analyses of humeral shapes in hadrosaurids (Ornithopoda, Dinosauria). *Senckenbergiana lethaea, 82*(1), 43-57.

Erickson, G. M., Rogers, K. C., & Yerby, S. A. (2001). Dinosaurian growth patterns and rapid avian growth rates. *Nature, 412*, 429-433.

Evans, D. C. (2010). Cranial anatomy and systematics of *Hypacrosaurus altispinus*, and a comparative analysis of skull growth in lambeosaurine hadrosaurids (Dinosauria: Ornithischia). *Zoological Journal of the Linnean Society, 159*(2), 398-434. doi:10.1111/j.1096-3642.2009.00611.x

Evans, D. C., Eberth, D. A., Ryan, M. l. J., & Therrien, F. (2015). Hadrosaurid (*Edmontosaurus*) bonebeds from the Horseshoe Canyon Formation (Horsethief Member) at Drumheller, Alberta, Canada: geology, preliminary taphonomy, and significance. *Canadian Journal of Earth Sciences, 52*(8), 642-654. doi:10.1139/cjes-2014-0184

Evans, D. C., Forster, C. A., & Reisz, R. R. (2005). The Type Specimen of *Tetragonosaurus erectofrons* (Ornithischia: Hadrosauridae) and the Identification of Juvenile Lambeosaurines. In P. J. Currie & E. B. Koppelhus (Eds.), *Dinosaur Provincial Park: a spectacular ancient ecosystem revealed* (pp. 349-366): Indiana University Press.

Evans, D. C., & Reisz, R. R. (2007). Anatomy and Relationships of *Lambeosaurus magnicristatus*, a crested hadrosaurid dinosaur (Ornithischia) from the Dinosaur Park Formation, Alberta. *Journal of Vertebrate Paleontology, 27*(2), 373-393. doi:10.1671/0272-4634(2007)27[373:Aarolm]2.0.Co;2

Evans, D. C., Reisz, R. R., & Dupuis, K. (2007). A juvenile Parasaurolophus (Ornithischia: Hadrosauridae) braincase from Dinosaur Provincial Park, Alberta, with comments on crest ontogeny in the genus. *Journal of Vertebrate Paleontology, 27*(3), 642-650. doi:10.1671/0272-4634(2007)27[642:Ajpohb]2.0.Co;2

855 Evans, D. C., Sues, H., Bavington, R., & Campione, N. E. (2009). An unusual hadrosaurid braincase from
856 the Dinosaur Park Formation and the biostratigraphy of Parasaurolophus (Ornithischia:
857 Lambeosaurinae) from southern Alberta. *Canadian Journal of Earth Sciences, 46*(11), 791-800.
858 doi:10.1139/e09-050
859 Fanti, F., Bell, P. R., & Sissons, R. L. (2013). A diverse, high-latitude ichnofauna from the Late Cretaceous
860 Wapiti Formation, Alberta, Canada. *Cretaceous Research, 41*, 256-269.
861 Fanti, F., & Catuneanu, O. (2009). Stratigraphy of the Upper Cretaceous Wapiti Formation, west-central
862 Alberta, Canada. *Canadian Journal of Earth Sciences, 46*(4), 263-286. doi:10.1139/e09-020
863 Fanti, F., & Catuneanu, O. (2010). Fluvial sequence stratigraphy: the Wapiti Formation, West-Central
864 Alberta, Canada. *Journal of Sedimentary Research, 80*(4), 320-338. doi:10.2110/jsr.2010.033
865 Fanti, F., Currie, P. J., & Burns, M. E. (2015). Taphonomy, age, and paleoecological implication of a new
866 *Pachyrhinosaurus* (Dinosauria: Ceratopsidae) bonebed from the Upper Cretaceous (Campanian)
867 Wapiti Formation of Alberta, Canada. *Canadian Journal of Earth Sciences, 52*(4), 250-260.
868 doi:10.1139/cjes-2014-0197
869 Fanti, F., & Miyashita, T. (2009). A high latitude vertebrate fossil assemblage from the Late Cretaceous of
870 west-central Alberta, Canada: evidence for dinosaur nesting and vertebrate latitudinal gradient.
871 *Palaeogeography, Palaeoclimatology, Palaeoecology, 275*(1-4), 37-53.
872 doi:10.1016/j.palaeo.2009.02.007
873 Farke, A. A., Chok, D. J., Herrero, A., Scolieri, B., & Werning, S. (2013). Ontogeny in the tube-crested
874 dinosaur *Parasaurolophus* (Hadrosauridae) and heterochrony in hadrosaurids. *PeerJ, 1*, e182.
875 doi:10.7717/peerj.182
876 Farlow, J. O. (1976). A consideration of the trophic dynamics of a Late Cretaceous large dinosaur
877 community (Oldman Formation). *Ecology, 57*, 841-857.

878 Fiorillo, A. R. (1988). Taphonomy of Hazard Homestead Quarry (Ogallala Group), Hitchcook County,
879 Nebraska. *Contributions to Geology, 26*(2), 57-97.
880 Fiorillo, A. R. (1998). Dental microwear patterns of the sauropod dinosaurs *Camarasaurus* and
881 *Diplodocus*: evidence for resource partitioning in the Late Jurassic of North America. *Historical*
882 *Biology, 13*, 1-16.
883 Forster, C. A. (1990). Evidence for juvenile groups in the ornithopod dinosaur *Tenontosaurus tilletti*
884 Ostrom. *Journal of Paleontology, 64*(1), 164-165.
885 Fowler, D. W. (2017). Revised geochronology, correlation, and dinosaur stratigraphic ranges of the
886 Santonian-Maastrichtian (Late Cretaceous) formations of the Western Interior of North America.
887 *PLoS One, 12*(11).
888 Funston, G. F., Currie, P. J., Eberth, D. A., Ryan, M. J., Chinzorig, T., Badamgarav, D., & Longrich, N. R.
889 (2016). The first oviraptorosaur (Dinosauria: Theropoda) bonebed: evidence of gregarious
890 behaviour in a maniraptoran theropod. *Scientific Reports, 6*(35782).
891 Galton, P. M. (1982). Juveniles of the stegosaurian dinosaur *Stegosaurus* from the Upper Jurassic of
892 North America. *Journal of Vertebrate Paleontology, 2*, 47-62.
893 Gangloff, R. A., & Fiorillo, A. R. (2010). Taphonomy and Paleoecology of a Bonebed from the Prince
894 Creek Formation, North Slope, Alaska. *Palaios, 25*(5-6), 299-317. doi:10.2110/palo.2009.p09-
895 103r
896 Gates, T. A., Sampson, S. D., De Jesús, C. R. D., Zanno, L. E., Eberth, D., Hernandez-Rivera, R., . . . Kirkland,
897 J. I. (2007). Velafrons coahuilensis, a new lambeosaurine hadrosaurid (Dinosauria: Ornithopoda)
898 from the late Campanian Cerro del Pueblo Formation, Coahuila, Mexico. *Journal of Vertebrate*
899 *Paleontology, 27*(4), 917-930. doi:10.1671/0272-4634(2007)27[917:Vcanlh]2.0.Co;2
900 Getty, M., Eberth, D. A., Brinkman, D. B., & Ryan, M. (1998). Taphonomy of three *Centrosaurus*
901 bonebeds in the Dinosaur Park Formation, Alberta. *Journal of Vertebrate Paleontology, 18*.

902 Gilmore, C. W. (1917). *Brachyceratops*, a ceratopsian dinosaur from the Two Medicine Formation of
903 Montana with notes on associated reptiles. *United States Geological Survey Professional Paper,*
904 *103*, 1-45.
905 Godefroit, P., Bolotsky, Y. L., & Van Itterbeeck, J. (2004). The lambeosaurine dinosaur Amurosaurus
906 riabinini, from the Maastrichtian of Far Eastern Russia. *Acta Palaeontologica Polonica*, 49(4).
907 Henderson, D. M. 2014. Duck soup: the floating fates of hadrosaurs and ceratopsians at Dinosaur
908 Provincial Park. Pp. 459–466 in D. A. Eberth and D. C. Evans, eds. *Hadrosaurs*. Indiana University
909 Press, Bloomington
910 Hill, A., & Behrensmeyer, A. K. (1984). Disarticulation patterns in some modern East African mammals.
911 *Palaeobiology, 10*(3), 366-376.
912 Hone, D. W., Sullivan, C., Zhao, Q., Wang, K., & Xu, X. (2014). Body size distribution in a death
913 assemblage of a colossal hadrosaurid from the Upper Cretaceous of Zhucheng, Shandong
914 Province, China. In D. A. Eberth & D. C. Evans (Eds.), *Hadrosaurs* (pp. 524-531). Bloomington:
915 Indiana University Press.
916 Horner, J. R. (1982). Evidence of colonial nesting and 'site fidelity' among ornithschian dinosaurs.
917 *Nature, 297*, 675-676.
918 Horner, J. R. (1983). Cranial Osteology and Morphology of the Type Specimen of *Maiasaura peeblesorum*
919 (Ornithischia: Hadrosauridae), with Discussion of Its Phylogenetic Position. *Journal of Vertebrate*
920 *Paleontology, 3*(1), 29-38.
921 Horner, J. R. (1992). Cranial morphology of *Prosaurolophus* (Ornithischia: Hadrosauridae) with
922 descriptions of two new hadrosaurid species and an evaluation of hadrosaurid phylogenetic
923 relationships. *Museum of the Rockies Occasional Paper, 2*, 1-119.
924 Horner, J. R. (1999). Egg clutches and embryos of two hadrosaurian dinosaurs. *Journal of Vertebrate*
925 *Paleontology, 19*(4), 607-611. doi:10.1080/02724634.1999.10011174

926 Horner, J. R., & Currie, P. J. (1994). Embryonic and neonatal morphology and ontogeny of a new species
927 of *Hypacrosaurus* (Ornithischia, Lambeosauridae) from Montana and Alberta. In K. Carpenter, K.
928 F. Hirsch, & J. R. Horner (Eds.), *Dinosaur Eggs and Babies* (pp. 312-336). Cambridge: University of
929 Cambridge.
930 Horner, J. R., De Ricqles, A., & Padian, K. (2000). Long bone histology of the hadrosaurid dinosaur
931 *Maiasaura peeblesorum* growth dynamics and physiology based on an ontogenetic series of
932 skeletal elements. *Journal of Vertebrate Paleontology, 20*(1), 115-129.
933 Horner, J. R., & Makela, R. (1979). Nest of juveniles provides evidence of family structure among
934 dinosaurs. *Nature, 282*(5736).
935 Horner, J. R., Ricqles, A. D., & Padian, K. (1999). Variation in skeletolochronology indicators: Implications
936 for age assessment and physiology. *Palaeobiology, 25*(3), 295-304.
937 Horner, J. R., Weishampel, D. B., & Forster, C. A. (2004). Hadrosauridae. In D. B. Weishampel, P. Dodson,
938 & H. Osmolska (Eds.), *The Dinosauria, second edition* (pp. 438-463). Berkeley: University of
939 California Press.
940 Hubner, T. R. (2012). Bone Histology in *Dysalotosaurus lettowvorbecki* (Ornithischia: Iguanodontia) –
941 Variation, Growth, and Implications. *PLoS One, 7*(1).
942 Hunt, R. M. (1978). Depositiona setting of a Miocene mammal assemblage, Sioux County, Nebraska
943 (U.S.A.). *Palaeogeography, Palaeoclimatology, Palaeoecology, 24*, 1-52.
944 Huttenlocker, A. K., Woodward, H. N., & Hall, B. K. (2013). *The Biology of Bone*. Berkeley: University of
945 California Press.
946 Jerzykiewicz, T., Currie, P. J., Eberth, D. A., Johnston, P. A., Koster, E. H., & Zheng, J. J. (1993). Djadokhta
947 Formation correlative strata in Chinese Inner Mongolia: an overview of the stratigraphy,
948 sedimentary geology, and paleontology and comparisons with the type locality in the pre-Altai
949 Gobi. *Canadian Journal of Earth Sciences, 30*(10), 2180-2195.

950 Keenan, S. W., & Scannella, J. B. (2014). Paleobiological implications of a *Triceratops* bonebed from the
951 Hell Creek Formation, Garfield County, northeastern Montana. In G. P. Wilson, W. A. Clemens, J.
952 R. Horner, & J. H. Hartman (Eds.), *Through the End of the Cretaceous in the Type Locality of the*
953 *Hell Creek Formation in Montana and Adjacent Areas* (Vol. 503): Geological Society of America.
954 Lehman, T. M. (2001). Late Cretaceous dinosaur provinciality. In D. H. Tanke & K. Carpenter (Eds.),
955 *Mesozoic vertebrate life* (pp. 310-328). Bloomington: Indiana University Press.
956 Lehman, T. M. (2006). Growth and Population Age Structure in the Horned Dinosaur *Chasmosaurus*. In K.
957 Carpenter (Ed.), *Horns and Beaks: Ceratopsian and Ornithopod Dinosaurs* (pp. 259-318).
958 Bloomington and Indianapolis: Indiana University Press.
959 Lucas, S. G., & Sullivan, R. M. (2006). The Kirtlandian land-vertebrate "age"–faunal composition,
960 temporal position and biostratigraphic correlation in the nonmarine Upper Cretaceous of
961 western North America. *New Mexico Museum of Natural History and Science Bulletin, 35*, 7-29.
962 Lucas, S. G., Sullivan, R. M., Lichtig, A. J., Dalman, S. G., & Jasinski, S. E. (2016). Late Cretaceous dinosaur
963 biogeography and endemism in the Western Interior Basin, North America: a critical re-
964 evaluation. *New Mexico Museum of Natural History and Science Bulletin, 71*, 195-213.
965 Lull, R. S., & Wright, N. E. (1942). Hadrosaurian Dinosaurs of North America. *Geological Society of*
966 *America – Special Papers, 40*.
967 Mallon, J. C., & Anderson, J. S. (2013). Skull Ecomorphology of Megaherbivorous Dinosaurs from the
968 Dinosaur Park Formation (Upper Campanian) of Alberta, Canada. *PLoS One, 8*(7).
969 Mallon, J. C., & Anderson, J. S. (2014). Implications of beak morphology for the evolutionary
970 paleoecology of the megaherbivorous dinosaurs from the Dinosaur Park Formation (upper
971 Campanian) of Alberta, Canada. *Palaeogeography Palaeoclimatology Palaeoecology, 394*, 29-41.

Mallon, J. C., Evans, D. C., Ryan, M. J., & Anderson, J. S. (2012). Megaherbivorous dinosaur turnover in the Dinosaur Park Formation (upper Campanian) of Alberta, Canada. *Palaeogeography, Palaeoclimatology, Palaeoecology, 350*, 124-138.

Mallon, J. C., Evans, D. C., Ryan, M. J., & Anderson, J. S. (2013). Feeding height stratification among the herbivorous dinosaurs from the Dinosaur Park Formation (upper Campanian) of Alberta, Canada. *BMC Ecol*.

Mathews, J., Henderson, M., & Williams, S. (2007). Taphonomy and sedimentology of the first known Triceratops bonebed, Carter County Montana. *Journal of Vertebrate Paleontology, 27*(3), 114a-114a. Retrieved from <Go to ISI>://WOS:000249535400378

McGarrity, C. T., Campione, N. E., & Evans, D. C. (2013). Cranial anatomy and variation inProsaurolophus maximus(Dinosauria: Hadrosauridae). *Zoological Journal of the Linnean Society, 167*(4), 531-568. doi:10.1111/zoj.12009

McWhinney, L., Matthias, A., & Carpenter, K. (2004). Corticated pressure erosions, or “pitting,” in osteodermal ankylosaur armor. *Journal of Vertebrate Paleontology, 24*, 92A.

Morris, W. J. (1970). Hadrosaurian dinosaur bills: morphology and function. *Los Angeles County Museum Contributions in Science, 193*.

Myers, T. S., & Fiorillo, A. R. (2009). Evidence for gregarious behavior and age segregation in sauropod dinosaurs. *Palaeogeography, Palaeoclimatology, Palaeoecology, 274*(1-2), 96-104. doi:10.1016/j.palaeo.2009.01.002

Norman, D. B. (1987). A mass-accumulation of vertebrates from the Lower Cretaceous of Nehden (Sauerland), West-Germany. *Proveedings of the Royal Society London Series B, 230*, 215-255.

Ostrom, J. H. (1961). Cranial Morphology of the Hadrosaurian Dinosaurs of North America. *Bulletin of the American Museum of Natural History, 122*, 35-186.

995 Ostrom, J. H. (1963). *Parasaurolophus cyrtocristatus:* A Crested Hadrosaurian Dinosaur from New
996 Mexico. *Chicago Natural History Museum, 14*(8).
997 Parks, W. A. (1922). *Parasaurolophus walkeri*: A New Genus and Species of Crested Trachodont
998 Dinosaur. *University of Toronto Studies, Geological Series, 13*, 1-32.
999 Pelletier, L., Chiaradia, A., Kato, A., & Ropert-Coudert, Y. (2016). Fine-scale spatial age segregation in the
1000 limited foraging area of an inshore seabird species, the little penguin. *Oecologia, 176*(2), 399-
1001 408.
1002 Peterson, J. E., Joseph, E., & Bigalke, C. L. (2013). Hydrodynamic Behaviours of Pachycephalosaurid
1003 Domes in Controlled Fluvial Settings: A Case Study in Experimental Dinosaur Taphonomy.
1004 *Palaios, 28*, 285-292. doi:10.2110/palo.2013.p13-003r
1005 Prieto-Márquez, A. (2010). Global phylogeny of hadrosauridae (Dinosauria: Ornithopoda) using
1006 parsimony and Bayesian methods. *Zoological Journal of the Linnean Society, 159*, 435-502.
1007 Prieto-Márquez, A. (2012). The skull and appendicular skeleton of *Gryposaurus latidens*, a saurolophine
1008 hadrosaurid (Dinosauria: Ornithopoda) from the early Campanian (Cretaceous) of Montana,
1009 USA. *Canadian Journal of Earth Sciences, 49*, 510-532.
1010 Prieto-Márquez, A., Chiappe, L. M., & Joshi, S. H. (2012). The Lambeosaurine Dinosaur *Magnapaulia*
1011 *laticaudus* from the Late Cretaceous of Baja California, Northwestern Mexico. *PLoS One, 7*(6),
1012 e38207. doi:10.1371/journal.pone.0038207
1013 Prieto-Márquez, A., & Gutarra, S. (2016). The 'duck-billed' dinosaurs of Careless Creek (Upper
1014 Cretaceous of Montana, USA), with comments on hadrosaurid ontogeny. *Journal of*
1015 *Paleontology, 90*(1), 133-146. Retrieved from https://doi.org/10.1017/jpa.2016.42
1016 Prieto-Márquez, A., & Norrell, M. A. (2010). Anatomy and Relationships of *Gilmoreosaurus mongoliensis*
1017 (Dinosauria: Hadrosauroidea) from the Late Cretaceous of Central Asia. *American Museum*
1018 *Novitates, 3694*.

1019 Raath, M. A. (1990). Morphological variation in small theropods and its meaning in systematics:
1020 evidence from *Syntarsus rhodesiensis*. In K. Carpenter & P. J. Currie (Eds.), *Dinosaur Systematics:*
1021 *Approaches and Perspectives* (pp. 92-105). Cambridge: Cambridge University Press.
1022 Rogers, R. R., Eberth, D. A., & Fiorillo, A. R. (2007). *Bonebeds: Genesis, Analysis, and Paleobiological*
1023 *Significance* (R. R. Rogers, D. A. Eberth, & A. R. Fiorillo Eds.). Chicago and London: The University
1024 of Chicago Press.
1025 Rogers, R. R., & Kidwell, M. (2007). A Conceptual Framework for the Genesis and Analysis of Vertebrate
1026 Skeletal Concentrations. In R. Rogers, D. Eberth, & A. Fiorillo (Eds.), *Bonebeds: Genesis, analysis,*
1027 *and paleobiological significance* (pp. 1-65). Chicago and London: The University of Chicago Press.
1028 Rothschild, B. M., Tanke, D., Rühli, F., Pokhojaev, A., & May, H. (2020). Suggested Case of Langerhans
1029 Cell Histiocytosis in a Cretaceous dinosaur. *Scientific Reports, 10*(2203), 1-10. Retrieved from
1030 https://doi.org/10.1038/s41598-020-59192-z
1031 Ryan, M. J., & Evans, D. C. (2005). Ornithischian Dinosaurs. In P. J. Currie & E. B. Koppelhus (Eds.),
1032 *Dinosaur Provincial Park: a spectacular ancient ecosystem revealed* (pp. 312-348). Bloomington:
1033 Inidana University Press.
1034 Sampson, S. D., Loewen, M. A., Farke, A. A., Roberts, E. M., Forster, C. A., Smith, J. A., & Titus, A. L.
1035 (2010). New Horned Dinosaurs from Utah Provide Evidence for Intracontinental Dinosaur
1036 Endemism. *PLoS One, 5*(9), e12292. doi:10.1371/journal.pone.0012292
1037 Scherzer, B. A., & Varricchio, D. J. (2010). Taphonomy of a Juvenile Lambeosaurine Bonebed from the
1038 Two Medicine Formation (Campanian) of Montana, United States. *Palaios, 25*(11-12), 780-795.
1039 doi:10.2110/palo.2009.p09-143r
1040 Slowiak, J., Szczygielski, T., Ginter, M., & Fostowicz-Frelik, Ł. (2020). Uninterrupted Growth in a Non-
1041 Polar Hadrosaur Explains the Gigantism Among Duck-Billed Dinosaurs. *Palaeontology*, 1-21.
1042 doi:10.1111/pala.12473

1043 Takasaki, R., Fiorillo, A. R., Kobayashi, Y., Tykoski, R. S., & McCarthy, P. J. (2019). The First Defnite
1044 Lambeosaurine Bone From the Liscomb Bonebed of the Upper Cretaceous Prince Creek
1045 Formation, Alaska, United States. *Scientific Reports, 9*(5384). Retrieved from
1046 https://doi.org/10.1038/s41598-019-41325-8
1047 Tanke, D., & Brett-Surman, M. K. (2001). Evidence of hatchling and nesting-size hadrosaurs (Reptilia:
1048 Ornithischia) from Dinosaur Provincial park (Dinosaur Park Formation: Campanian), Alberta.
1049 *Mesozoic vertebrate life*.
1050 Tanke, D. H. (2004). Mosquitoes and Mud: The 2003 Royal Tyrrell Museum Expedition to the Grande
1051 Prairie Region (northwestern Alberta, Canada). *Alberta Palaeontological Society Bulletin, 19*(2),
1052 3-31.
1053 Thorbjarnarson, J. B., & Hernandez, G. (1993). Reproductive ecology of the Orinoco crocodile
1054 (Crocodylus intermedius) in Venezuela. *Journal of herpetology*, 363-370.
1055 Ullmann, P. V., Shaw, A., Nellermoe, R., & Lacovara, K. J. (2017). Taphonomy of the Standing Rock
1056 Hadrosaur Site, Corson County, South Dakota. *Palaios, 32*(12), 779-796.
1057 doi:10.2110/palo.2017.060
1058 Vanderven, E., Burns, M. E., & Currie, P. J. (2014). Histologic growth dynamic study of *Edmontosaurus*
1059 *regalis* (Dinosauria: Hadrosauridae) from a bonebed assemblage of the Upper Cretaceous
1060 Horseshoe Canyon Formation, Edmonton, Alberta, Canada. *Canadian Journal of Earth Sciences,*
1061 *51*(11), 1023-1033. doi:10.1139/cjes-2014-0064
1062 Varricchio, D. J. (1995). Taphonomy of Jacks-Birthday Site, a Diverse Dinosaur Bonebed from the Upper
1063 Cretaceous Two-Medicine Formation of Montana. *Palaeogeography Palaeoclimatology*
1064 *Palaeoecology, 114*(2-4), 297-323. doi:Doi 10.1016/0031-0182(94)00084-L
1065 Varricchio, D. J. (2011). A distinct dinosaur life history? *Historical Biology, 23*(1), 91-107.
1066 doi:10.1080/08912963.2010.500379

1067 Varricchio, D. J., & Horner, J. R. (1993). Hadrosaurid and lambeosaurid bone beds from the Upper
1068 Cretaceous Two Medicine Formation of Montana: taphonomic and biologic implications.
1069 *Canadian Journal of Earth Sciences, 30*(5), 997-1006.
1070 Varricchio, D. J., Sereno, P. C., Xijin, Z., Lin, T., Wilson, J. A., & Lyon, G. H. (2008). Mud-Trapped Herd
1071 Captures Evidence of Distinctive Dinosaur Sociality. *Acta Palaeontologica Polonica, 53*(4), 567-
1072 578. doi:10.4202/app.2008.0402
1073 Vila, B., Sellés, A. G., & Brusatte, S. L. (2016). Diversity and faunal changes in the latest Cretaceous
1074 dinosaur communities of southwestern Europe. *Cretaceous Research, 57*, 552-564.
1075 Voorhies, M. (1969). *Taphonomy and Population Dynamics of an Early Pliocene Vertebrate Fauna, Knox*
1076 *County, Nebraska*. Laramie: University of Wyoming.
1077 Wiman, C. (1931). *Parasaurolophus tubicens* n. sp. aus der kreide in New Mexico. *Nova Acta Regiae*
1078 *Societatis Scietiarum Upsaliensis Ser IV, 7*, 11.
1079 Wosik, M., Chiba, K., Therrien, F., & Evans, D. C. (2020). Testing size–frequency distributions as a
1080 method of ontogenetic aging: a life-history assessment of hadrosaurid dinosaurs from the
1081 Dinosaur Park Formation of Alberta, Canada, with implications for hadrosaurid paleoecology.
1082 *Paleobiology*, 46(3), 379-404.
1083 Woodward, H. N., Freedman Fowler, E. A., Farlow, J. O., & Horner, J. R. (2015). *Maiasaura*, a model
1084 organism for extinct vertebrate population biology: a large sample statistical assessment of
1085 growth dynamics and survivorship. *Paleobiology, 41*(4), 503-527.
1086 Xing, H., Mallon, J. C., & Currie, M. L. (2017). Supplementary cranial description of the types of
1087 *Edmontosaurus regalis* (Ornithischia: Hadrosauridae), with comments on the phylogenetics and
1088 biogeography of Hadrosaurinae. *PLoS One, 12*(4), e0175253. Retrieved from https://doi.org/
1089 10.1371/journal.pone.0175253

Zanno, L., & Erickson, G. (2006). Ontogeny and life history of *Falcarius utahensis*, a primitive therizinosauroid from the Early Cretaceous of Utah. *Journal of Vertebrate Paleontology, 26*(3), 143A.

Zhao, Q., Benton, M. J., Xu, X., & Sander, P. M. (2014). Juvenile-only clusters and behaviour of the Early Cretaceous dinosaur *Psittacosaurus*. *Acta Palaeontologica Polonica, 59*(4), 827-834.

Zubalich, R., Capozzi, R., Fanti, F., & Catuneanu, O. (2021). Evolution of the Western Interior Seaway in west-central Alberta (late Campanian, Canada): Implications for hydrocarbon exploration. *Marine and Petroleum Geology*, 124, 104779.

Table Captions

Table 1. List of humeri recovered from the Spring Creek Bonebed as seen in Figure 4.

Table 2. Inventory and categorization of bones in a complete juvenile hadrosaurid skeleton and expected vs observed proportions of Voorhies groups from the Spring Creek Bonebed. Expected proportions were adapted from a variety of sources (Varricchio 1995; Horner et al., 2004; Scherzer & Varricchio, 2010; Bell & Campione, 2014). Observed proportions were calculated from the number of identifiable specimens.

Table 3. Comparison between lambeosaurine cranial bones founds at the Spring Creek Bonebed and other juvenile lambeosaurines. Morphological comparisons are based on the following specimens: *Corythosaurus casuarius*: ROM 759 from (Evans et al., 2005); *Hypacrosaurus altispinus*: CMN 2247 from (Brink et al., 2011); *Hypacrosaurus stebingeri*: TMP.1994.385.01, TCMI 2001.96.02, and NSM-PV 20377 from (Evans, 2010); *Kazaklambia convincens*: PIN2230/1 from Bell and Brink (2013); *Lambeosaurus* sp.: ROM 758 from (Brink et

al., 2011); *Parasaurolophus* sp.: RAM 14000 from (Farke et al., 2013); *Velafrons coahuliensis*: CPC-59 from (Gates et al., 2007).

Table 4. Postcranial elements from the Spring Creek lambeosaurine scaled against elements from a complete *Lambeosaurus* sp. (AMNH 5340; from Farke et al., 2013) to estimate total body length.

Table 5. Taphonomic observations from the Spring Creek Bonebed, including the results of Chi-squared tests on the number of prepared specimens.

Figure Captions

Figure 1. Locality map of main macrofossil localities from the Grande Prairie area and the geographic extent of the Wapiti Formation. (A) Locality map of the main macrofossil localities proximate to Grande Prairie, Alberta, Canada. Numbers indicate the following localities: 1) George Robinson Bonebed (Tanke, 2004); 2) Mummified *Edmontosaurus regalis* skeleton (Bell et al., 2014a); 3) Red Willow hadrosaur (Bell et al., 2014b); 4) Wapiti River *Pachyrhinosaurus* Bonebed (Fanti et al., 2015); 5) Pipestone Creek *Pachyrhinosaurus lakustai* Bonebed (Currie et al., 2008b); 6) Spring Creek Bonebed (red star; this study). (B) Map illustrating the lateral extent of the Wapiti Formation (in grey) across Alberta and into eastern British Columbia.

Figure 2. Quarry map of the Spring Creek Bonebed. (A) Map of the 2018 and 2019 excavations of the Spring Creek Bonebed by the Boreal Alberta Dinosaur Project (grey: isolated specimens; white: specimens in concretions). (B) Associated dentary (UALVP 59898), partial dental battery (UALVP 59887), and predentary (UALVP 59888) from Spring Creek Bonebed.

Reconstruction based on *Hypacrosaurus stebingeri* (Brink et al., 2011). The 10 cm scale bar applies to the bones in B and the skull reconstruction. (C) A rose diagram of the recorded orientations of long bones from the Spring Creek Bonebed showing a preferential NE–SW modality, but overall high circular variance. (D) Quarry photo of bones in situ.

Figure 3. Exposures at the Spring Creek Bonebed. (A) Photograph of the bank exposure at the Spring Creek Bonebed (indicated by white arrows). (B) Stratigraphic column from the Spring Creek Bonebed (sediment grains sizes: c, clay; m, mud; fs, fine sand; s, sand). Derek Larson (175 cm) for scale.

Figure 4. Right (top) and left (bottom) humeri recovered from the Spring Creek Bonebed and denoting the minimum number of individuals (MNI=eight) and their consistent size. Humeri show the typical lack of weathering and abrasion observed throughout the Spring Creek Bonebed. Additionally, humeri exhibit a variety of fracture styles and diagenetic distortion, causing the visible morphological variances. Note that letters correspond to Table 1. Humeri denoted with an asterisk were sectioned for histological analyses.

Figure 5. Left lambeosaurine premaxilla (UALVP 60537) from the Spring Creek Bonebed. (A) Lateral view, including life reconstruction based on *Hypacrosaurus stebingeri* (Brink et al., 2011). Grey region indicates the portion of the premaxilla that was preserved. (B) Dorsal view with a dashed white line indicating the perimeter of the exposed bony naris. Abbreviations: bn, bony naris; cdp, caudodorsal process; nv, nasal vestibule; om, oral margin.

Figure 6. Right lambeosaurine maxilla (UALVP 59881b) from the Spring Creek Bonebed. (A) Lateral view, showing hypothetical reconstruction based on *Hypacrosaurus* sp. (MOR 553s). The dashed white line indicates the anterior margin of the sutural surface for the jugal. Black

arrows indicate the location of lateral foramina. (B) Medial view. (C) Anterodorsal view. (D) Dorsal view. (E) Anterior cross section and schematic showing three internal teeth and one erupted tooth. (F) Ventral view. Abbreviations: af, alveolar foramina; df, dorsal foramen; dp, dorsal process; ec, ectopterygoid ridge; mt, maxillary teeth; ps, premaxillary shelf; sdf, secondary dorsal foramen; ssj, sutural surface for the jugal.

Figure 7. Left lambeosaurine postorbital (UALVP 59902) from the Spring Creek Bonebed. (A) Dorsolateral view. (B) Ventromedial view. White dashed line outlines the shape of the latersphenoid fossa. Note the longitudinal fracture on the medial surface in (B), which could also represent a neurovascular canal. Abbreviations: jp, jugal process; or, orbital rim; sp, squamosal process; ssf, sutural surface for frontal; ssp, sutural surface for parietal; sspf, sutural surface for prefrontal.

Figure 8. Thin sections of Spring Creek Bonebed humeri showing bone microstructure. (A) Thin section of a humerus (UALVP 60539) showing the typical bone microstructure of humeri from the Spring Creek Bonebed, as described in the text. Scale bar = 1 mm. White arrows: 1, cancellous bone; 2, reticular bone; 3, plexiform bone; 4, laminar bone; 5, Haversian bone. (B) Laminar bone from UALVP 60533. Scale bar = 500 μm. (C) Reticular bone from UALVP 60535. Scale bar = 500 μm. (D) Plexiform bone from UALVP 60535. Scale bar = 500 μm. (E) Haversian reconstruction from UALVP 60539. Scale bar = 500 μm.

Figure 9. Examples of bone modification from the Spring Creek Bonebed. (A) Unhealed parallel toothmarks (white arrows) on the lateral surface of the left dentary (UALVP 59907) interpreted as post mortem scavenging. (B) Pathology (margin indicated by white arrows) on the lateral surface of the supra-acetabular process (sa) from an incomplete ilium (UALVP 60540). (C) Example of paralell striae on the diaphysis of a fibula (UALVP 59982).

Figure 10. Biostratigraphy and palaeobiogeography of temporally and spatially proximate Lambeosaurinae from Alberta, Canada, Montana, USA, and Mexico. (A) Biostratigraphic distribution of Lambeosaurinae across strata from northwestern (Fanti & Catuneanu, 2009; this study) and southern Alberta, Canada (Mallon et al., 2012; Eberth et al., 2013; Eberth & Kamo, 2020), Montana, USA (Horner & Currie, 1994; Campbell et al., 2019), western and northeastern Mexico (Lucas & Sullivan, 2006; Gates et al., 2007; Prieto-Márquez et al., 2012; Fowler, 2017). The Wapiti and Horseshoe Canyon formations are subdivided into units and members, respectively. Grey strata represent marine formations. The dashed error ranges for the Spring Creek lambeosaurines represents a temporal range within Unit 3, between the Pipestone Creek Bonebed (~73.5 Ma; Currie et al., 2008b) and the basal-most Horseshoe Canyon Formation (~74.4 Ma; Eberth & Braman, 2012). (B) Paleobiogeographical distribution of Lambeosaurinae across Montana, USA, Alberta, Canada, and Mexico (Lull & Wright, 1942; Horner & Currie, 1994; Evans & Reisz, 2007; Evans et al., 2007; Gates et al., 2007; Evans et al., 2009; Evans, 2010; Prieto-Márquez et al., 2012). The silhouette of the Spring Creek lambeosaurine and *Magnapaulia laticaudus* were created by Scott Hartman and Dmitry Bogdanov, respectively. Both were vectorized by T. Michael Keesey and used under the creative commons attribution 3.0 unported license (https://creativecommons.org/licenses/by/3.0/). The remaining silhouettes were used and modified under the public domain dedication 1.0 license. All silhouettes were sourced from www.phylopic.org.

Supplementary Figure Captions

Supplementary Figure 1. Additional images of humeri thin sections from the Spring Creek Bonebed. (A) UALVP 60534. (B) UALVP 60537. (C) UALVP 60536. Scale bars represent 500 μm.

Supplementary Figure 2. Additional images of humeri thin sections from the Spring Creek Bonebed. (A) UALVP 60533. (B) UALVP 60532. (C) TMP 1988.94.0006. (D) TMP 1991.137.0009. White scale bars in (A) and (B) represent 500 μm.

Supplementary Figure 3. Additional images of humeri thin sections from the Spring Creek Bonebed. (A) UALVP 60533. (B) UALVP 60539. (C) UALVP 60532.

Table 1(on next page)

List of humeri recovered from the Spring Creek Bonebed as seen in Figure 4.

Table 1. List of humeri recovered from the Spring Creek Bonebed as seen in Figure 4.

Institutional abbreviations: UoA, University of Alberta, Edmonton, Canada; UNE, University of New England, Armidale, Australia.

Figure Identifier	Specimen Number	Element	Length (mm)	Sectioning Institution
A	TMP 1991.137.0005	Right humerus (proximal)	282*	
B	UALVP 60537	Right humerus	261	UoA
C	UALVP 60539	Right humerus	247	UoA
D	UALVP 60534	Right humerus	246**	UoA
E	UALVP 60536	Right humerus	262**	UoA
F	UALVP 60532	Right humerus (distal)	268*	UoA
G	UALVP 60535	Right humerus (proximal)	252*	
H	UALVP 60541	Right humerus (proximal)	270*	
I	TMP 1991.127.0001	Left humerus	253	
J	UALVP 60533	Left humerus (distal)	231*	UoA
K	TMP 1991.137.0009	Left humerus (distal)	279*	UNE
L	TMP 1988.94.0002	Left humerus (distal)	235*	
M	TMP 1988.94.0006	Left humerus (distal)	254*	UNE
	Humerus length:	Mean = 257mm	sd = 15.5mm	

*Estimated lengths

**Have undergone diagenetic modification

Table 2(on next page)

Inventory and categorization of bones in a complete juvenile hadrosaurid skeleton and expected vs observed proportions of Voorhies groups from the Spring Creek Bonebed.

Expected proportions were adapted from a variety of sources (Varricchio 1995; Horner et al., 2004; Scherzer & Varricchio, 2010; Bell & Campione, 2014). Observed proportions were calculated from the number of identifiable specimens.

Table 2. Inventory and categorization of bones in a complete juvenile hadrosaurid skeleton and expected vs observed proportions of Voorhies groups from the Spring Creek Bonebed.

Expected proportions were adapted from a variety of sources (Varricchio 1995; Horner et al., 2004; Scherzer & Varricchio, 2010; Bell & Campione, 2014). Observed proportions were calculated from the number of identifiable specimens.

Voorhies Group I			Voorhies Group II			Voorhies Group III		
Category	**Element**	**Count**	**Category**	**Element**	**Count**	**Category**	**Element**	**Count**
Light cranial elements	Premaxillae	2	Pectoral elements	Sternal plates	2	Limb bones	Humeri	2
	Nasals	2		Coracoids	2		Radii	2
	Lacrimals	2		Scapulae	2		Ulnae	2
	Jugals	2	Dense cranial elements	Maxillae	2		Femora	2
	Quadratojugals	2		Dentaries	2		Tibiae	2
	Postorbitals	2		Braincase	1		Fibulae	2
	Surangulars	2	Tarsals and metapodials	Astragali	2			
	Exoccipitals	2		Metatarsals	6			
	Hyoids	2		Metacarpals	6			
	Squamosals	2						
	Quadrates	2						
	Frontals	2						
	Ectopterygoids	2						
Digital elements	Pedal phalanges	24						
	Manual phalanges	24						
Ribs	Dorsal ribs	36						
Vertebrae (including isolated centra)	Cervical	13						
	Dorsal	18						
	Caudal	50						
	Sacral	9						
Vertebral processes	Transverse processes	84						
	Neural spines	49						
	Haemal arches	35						
	Expected proportion	89.6%		Expected proportion	7.5%		Expected proportion	2.9%
	Observed proportion	48%		Observed proportion	23.3%		Observed proportion	28.7%
Chi-squared results:	X-squared = 41.746							
	df = 2							
	p-value << 0.001							

Table 3(on next page)

Comparison between lambeosaurine cranial bones founds at the Spring Creek Bonebed and other juvenile lambeosaurines.

Morphological comparisons are based on the following specimens: *Corythosaurus casuarius*: ROM 759 from (Evans et al., 2005); *Hypacrosaurus altispinus*: CMN 2247 from (Brink et al., 2011); *Hypacrosaurus stebingeri*: TMP.1994.385.01, TCMI 2001.96.02, and NSM-PV 20377 from (Evans, 2010); *Kazaklambia convincens*: PIN2230/1 from Bell and Brink (2013); *Lambeosaurus* sp.: ROM 758 from (Brink et al., 2011); *Parasaurolophus* sp.: RAM 14000 from (Farke et al., 2013); *Velafrons coahuliensis*: CPC-59 from (Gates et al., 2007).

Table 3. Comparison between lambeosaurine cranial bones founds at the Spring Creek Bonebed and other juvenile lambeosaurines. Morphological comparisons are based on the following specimens: *Corythosaurus casuarius*: ROM 759 from (Evans et al., 2005); *Hypacrosaurus altispinus*: CMN 2247 from (Brink et al., 2011); *Hypacrosaurus stebingeri*: TMP.1994.385.01, TCMI 2001.96.02, and NSM-PV 20377 from (Evans, 2010); *Kazaklambia convincens*: PIN2230/1 from Bell and Brink (2013); *Lambeosaurus* sp.: ROM 758 from (Brink et al., 2011); *Parasaurolophus* sp.: RAM 14000 from (Farke et al., 2013); *Velafrons coahuliensis*: CPC-59 from (Gates et al., 2007).

Spring Creek Lambeosaurine Morphologies	*Corythosaurus casuarius*	*Hypacrosaurus altispinus*	*Hypacrosaurus stebingeri*	*Kazaklambia convincens*	*Lambeosaurus* sp.	*Parasaurolophus* sp.	*Velafrons coahuliensis*
Premaxilla							
No ventrolateral tab-like process	NA	No	No	NA	Yes	No	No
Bony naris attenuates anterior to crest snout angle	No	Yes	No	NA	Yes	NA	Yes
Crest-snout angle ~158°	~155°	~169°	~150°*	NA	~156°	~162°*	~157°
Maxilla							
Dorsal opening foramen	NA	Yes	NA	NA	NA	NA	Yes
Secondary dorsal foramen	Yes	NA	NA	NA	NA	NA	NA
Anterodorsal angle ~151°	~149°	~147°	~143°*	NA	~154°	~165°*	~144°
Postorbital							
No prefrontal contact doming	Yes	Yes	Yes	No	Yes	Yes	Yes

Arcuate antorbital fenestra margin	Yes	No	Yes	No	No	No	No
Bifurcated squamosal process	Yes	No	Yes	Yes	Yes	Yes	Yes

*Measured from reconstructions

Table 4(on next page)

Postcranial elements from the Spring Creek lambeosaurine scaled against elements from a complete *Lambeosaurus* sp. (AMNH 5340; from Farke et al., 2013) to estimate total body length.

Table 4. Postcranial elements from the Spring Creek lambeosaurine scaled against elements from a complete *Lambeosaurus* sp. (AMNH 5340; from Farke et al., 2013) to estimate maximum total body length.

Taxon	*Lambeosaurus* sp. (Farke et al., 2013)	Lambeosaurinae indet. (this study)	Ratio of Spring Creek Specimens to AMNH 5340
Specimen	AMNH 5340	Longest Spring Creek specimens	
Humerus length (mm)	305	261 UALVP 60537	0.86
Femur length (mm)	590	558 BADP 2019.0813.03**	0.94
Tibia length (mm)	550	547 TMP.1995.024.0002	0.99
Fibula length (mm)	530	455 TMP.1991.137.17	0.86
Total Length (m)	4.31	≤ 4.27*	

Brackets indicate scale factor from AMNH 5340

*Estimated body length

**Based on field measurements of unprepared specimens

Table 5(on next page)

Taphonomic observations from the Spring Creek Bonebed, including the results of Chi-squared tests on the number of prepared specimens.

Table 5. Taphonomic observations from the Spring Creek Bonebed, including the results of Chi-squared tests on the number of prepared specimens.

Weathering Stage (Behrensmeyer, 1978; Fiorillo, 1988)	**Observed proportion**	**Abrasion Stage** (Fiorillo, 1988)	**Observed proportion**	**Fracture Style**	**Observed proportion**
Stage 0: No signs of cracking or flaking on bone. Possible years exposed after death: 0-1	72.9%	**Stage 0:** Bone is unabraded, preserving all processes and edges.	84.3%	**Complete:** Bone is preserved in its entirety.	44.2%
Stage 1: Bone is beginning to show signs of longitudinal cracking. Possible years exposed after death: 0-3	16.8%	**Stage 1:** Slight abrasion with some rounding of edges.	13.9%	**Spiral:** Fractures with irregular fracture surfaces preserved from pre-burial.	7.6%
Stage 2: Thin layers of bone flaking, typically associated with longitudinal cracks. Possible years exposed after death: 2-6	10.3%	**Stage 2:** Moderate abrasion in which edges are well-rounded, and processes may or may not be identifiable.	0.9%	**Transverse:** Straight, transverse fractures preserved from post burial.	9.3%
Stage 3: Patches of exposed fibrous texture where concentrically layered bone has been removed. Possible years exposed after death: 4-15+	0%	**Stage 3:** High level of abrasion, edges extremely rounded, original bone shape is barely recognisable.	0.9%	**Mixed:** Both transverse and spiral fractures preserved.	38.9%
Chi-squared results: $X^2 = 71.08$ p-value <<0.001		Chi-squared results: $X^2 = 191.77$ p-value <<0.001		Chi-squared results: $X^2 = 44.538$ p-value <<0.001	
Proportion of specimens observed with toothmarks: 3.8%				Proportion of specimens observed with parallel striae: 28.2%	

Figure 1

Locality map of main macrofossil localities from the Grande Prairie area and the geographic extent of the Wapiti Formation.

(A) Locality map of the main macrofossil localities proximate to Grande Prairie, Alberta, Canada. Numbers indicate the following localities: 1) George Robinson Bonebed (Tanke, 2004); 2) Mummified *Edmontosaurus regalis* skeleton (Bell et al., 2014a); 3) Red Willow hadrosaur (Bell et al., 2014b); 4) Wapiti River *Pachyrhinosaurus* Bonebed (Fanti et al., 2015); 5) Pipestone Creek *Pachyrhinosaurus lakustai* Bonebed (Currie et al., 2008b); 6) Spring Creek Bonebed (red star; this study). (B) Map illustrating the lateral extent of the Wapiti Formation (in grey) across Alberta and into eastern British Columbia.

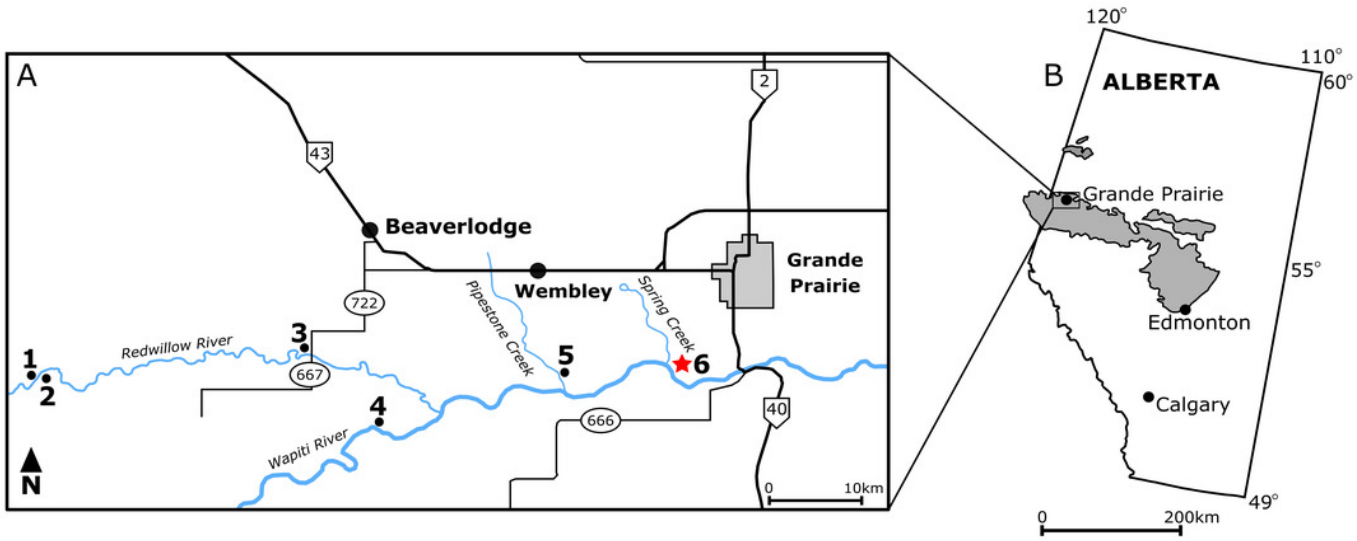

Figure 2

Quarry map of the Spring Creek Bonebed.

(A) Map of the 2018 and 2019 excavations of the Spring Creek Bonebed by the Boreal Alberta Dinosaur Project (grey: isolated specimens; white: specimens in concretions). (B) Associated dentary (UALVP 59898), partial dental battery (UALVP 59887), and predentary (UALVP 59888) from Spring Creek Bonebed. Reconstruction based on *Hypacrosaurus stebingeri* (Brink et al., 2011). The 10 cm scale bar applies to the bones in B and the skull reconstruction. (C) A rose diagram of the recorded orientations of long bones from the Spring Creek Bonebed showing a preferential NE–SW modality, but overall high circular variance. (D) Quarry photo of bones in situ.

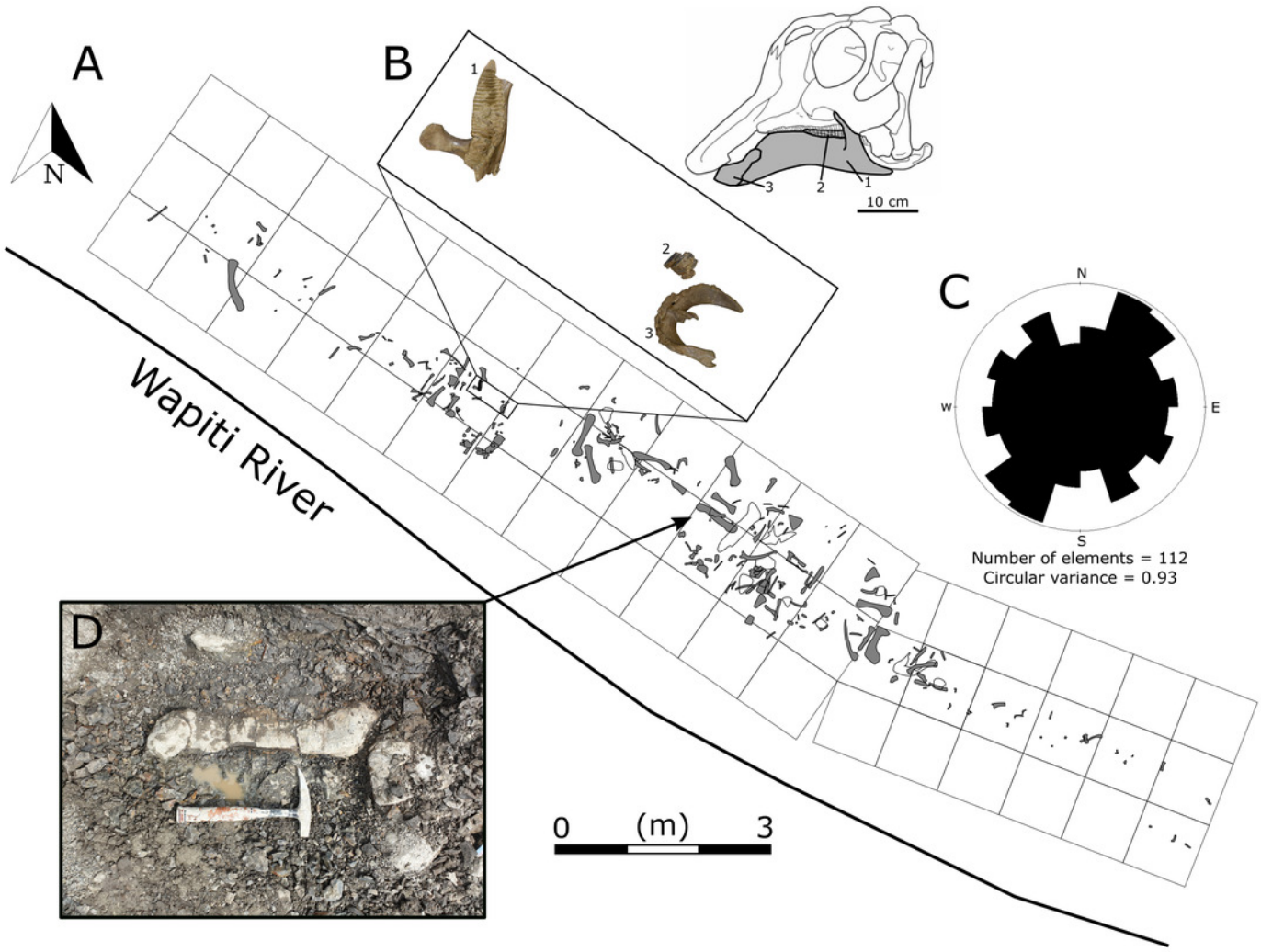
A
N
B
1
2
3
10 cm
Wapiti River
C
N
W
E
S
Number of elements = 112
Circular variance = 0.93
D
0 (m) 3

Figure 3

Exposures at the Spring Creek Bonebed.

(A) Photograph of the bank exposure at the Spring Creek Bonebed (indicated by white arrows). (B) Stratigraphic column from the Spring Creek Bonebed (sediment grains sizes: c, clay; m, mud; fs, fine sand; s, sand). Derek Larson (175 cm) for scale.

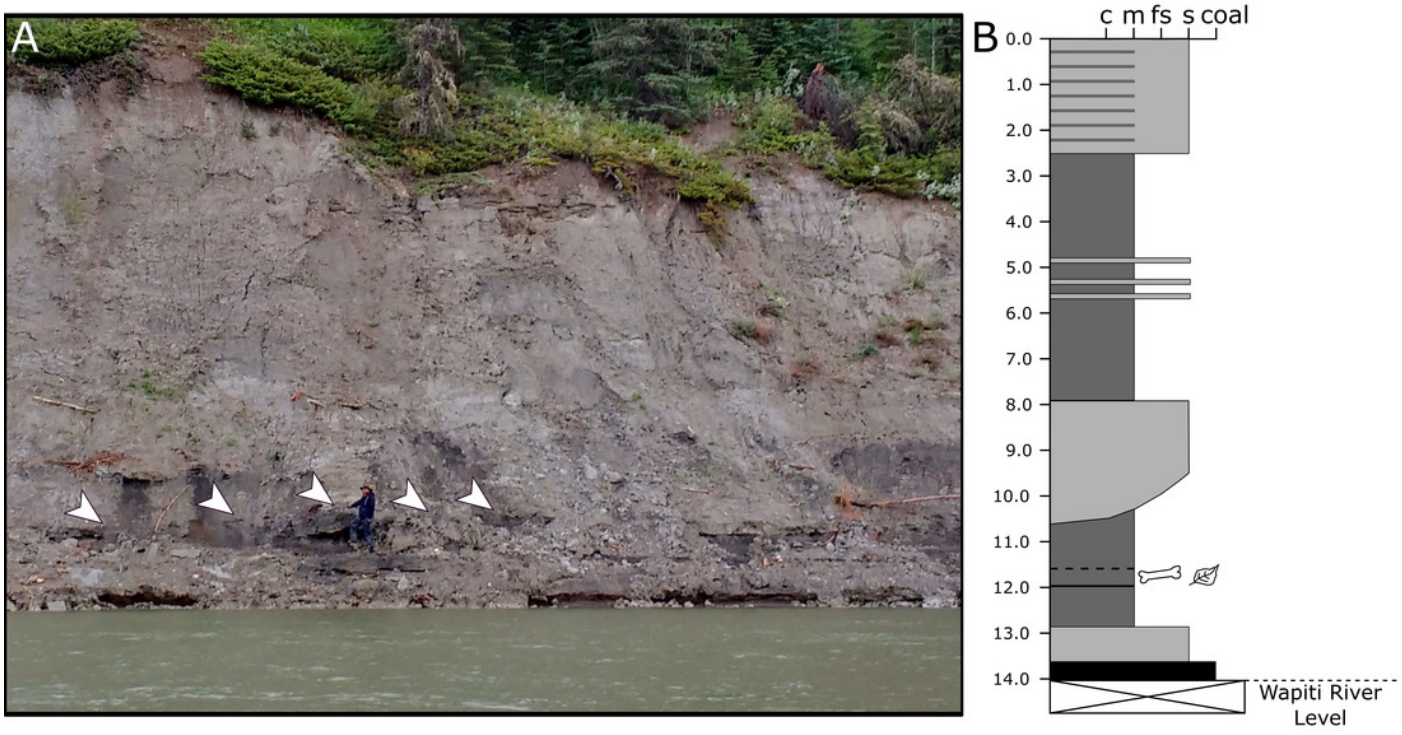

Figure 4

Right (top) and left (bottom) humeri recovered from the Spring Creek Bonebed and denoting the minimum number of individuals (MNI=eight) and their consistent size.

Humeri show the typical lack of weathering and abrasion observed throughout the Spring Creek Bonebed. Additionally, humeri exhibit a variety of fracture styles and diagenetic distortion, causing the visible morphological variances. Note that letters correspond to Table 1. Humeri denoted with an asterisk were sectioned for histological analyses.


A
B*
C*
D*
E*
F*
G
H
10 cm
I
J*
K*
L
M*

Figure 5

Left lambeosaurine premaxilla (UALVP 60537) from the Spring Creek Bonebed.

(A) Lateral view, including life reconstruction based on *Hypacrosaurus stebingeri* (Brink et al., 2011). Grey region indicates the portion of the premaxilla that was preserved. (B) Dorsal view with a dashed white line indicating the perimeter of the exposed bony naris. Abbreviations: bn, bony naris; cdp, caudodorsal process; nv, nasal vestibule; om, oral margin.

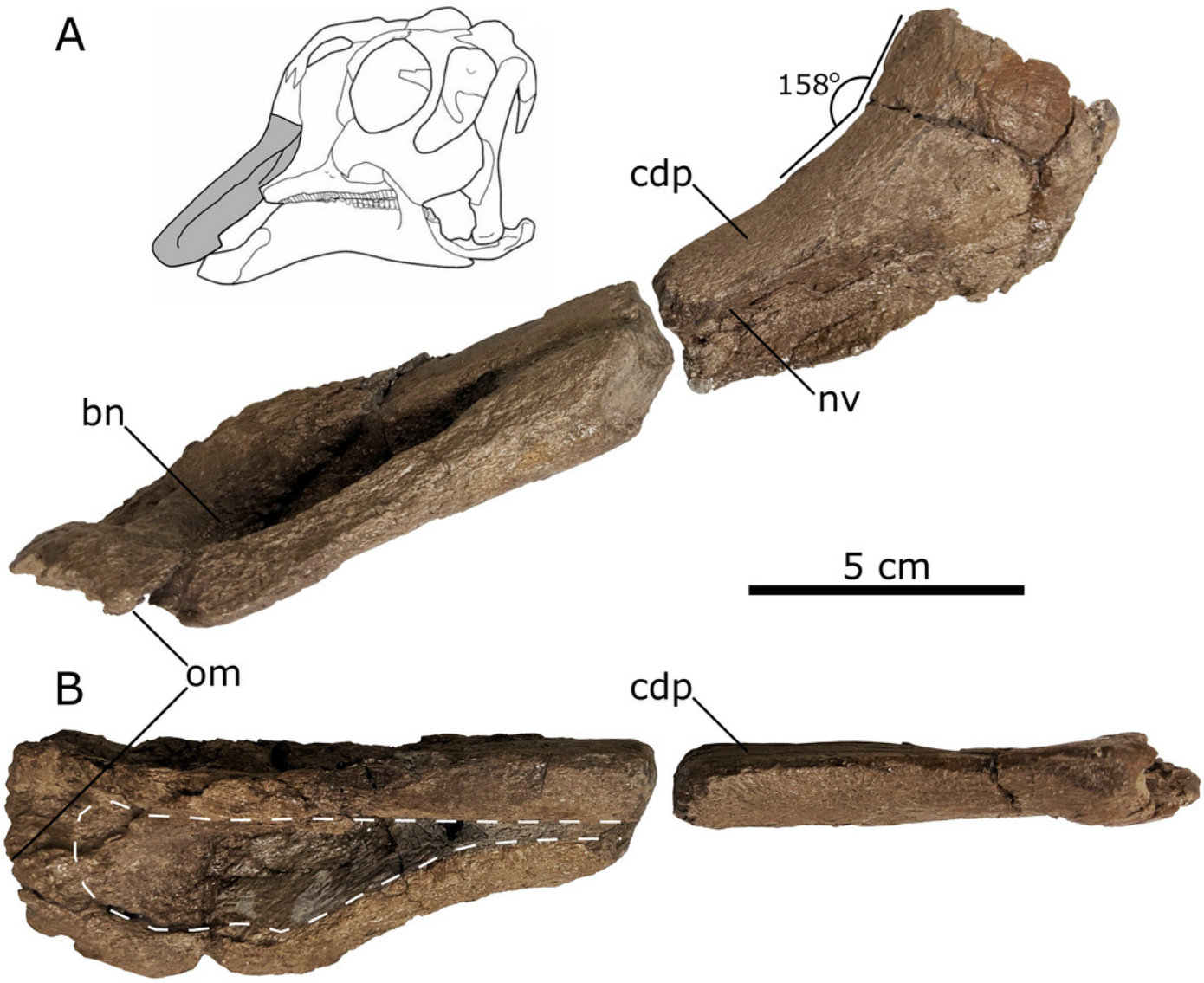

Figure 6

Right lambeosaurine maxilla (UALVP 59881b) from the Spring Creek Bonebed.

(A) Lateral view, showing hypothetical reconstruction based on *Hypacrosaurus* sp. (MOR 553s). The dashed white line indicates the anterior margin of the sutural surface for the jugal. Black arrows indicate the location of lateral foramina. (B) Medial view. (C) Anterodorsal view. (D) Dorsal view. (E) Anterior cross section and schematic showing three internal teeth and one erupted tooth. (F) Ventral view. Abbreviations: af, alveolar foramina; df, dorsal foramen; dp, dorsal process; ec, ectopterygoid ridge; mt, maxillary teeth; ps, premaxillary shelf; sdf, secondary dorsal foramen; ssj, sutural surface for the jugal.

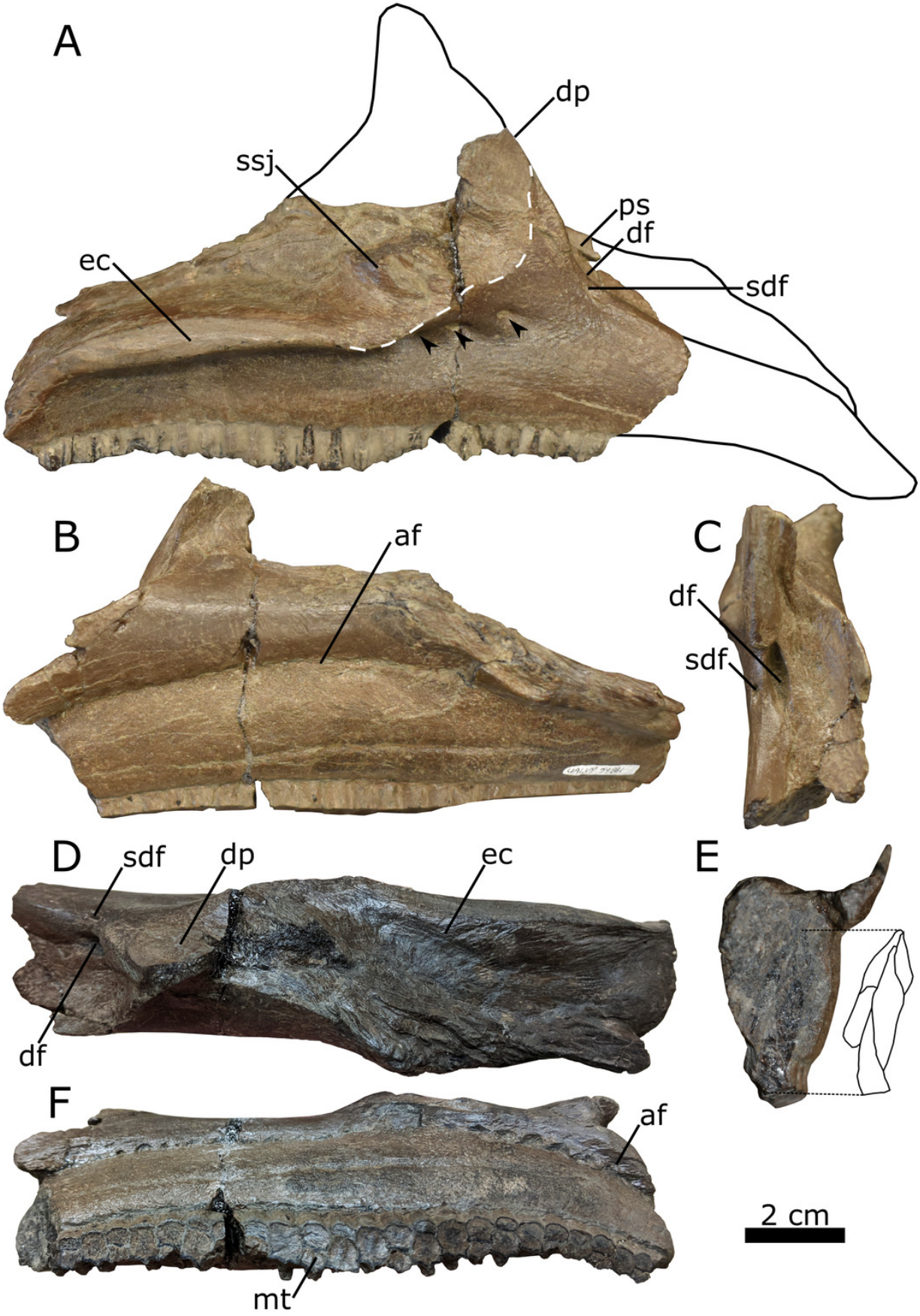
A
dp
ssj
ps
df
ec
sdf
B
af
C
df
sdf
D
sdf
dp
ec
df
E
F
af
mt
2 cm

Figure 7

Left lambeosaurine postorbital (UALVP 59902) from the Spring Creek Bonebed.

(A) Dorsolateral view. (B) Ventromedial view. White dashed line outlines the shape of the latersphenoid fossa. Note the longitudinal fracture on the medial surface in (B), which could also represent a neurovascular canal. Abbreviations: jp, jugal process; or, orbital rim; sp, squamosal process; ssf, sutural surface for frontal; ssp, sutural surface for parietal; sspf, sutural surface for prefrontal.

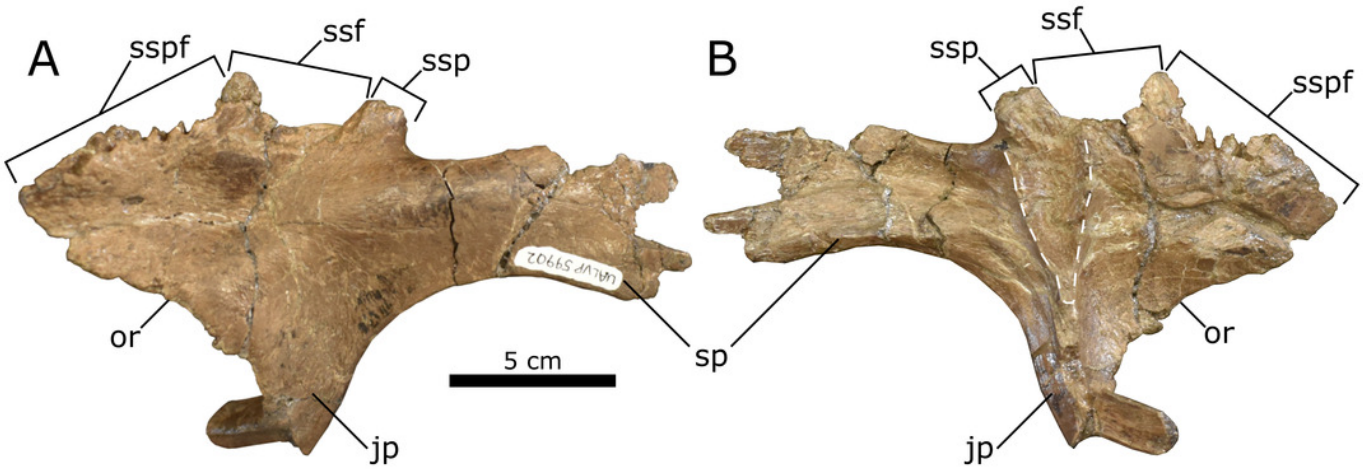

Figure 8

Thin sections of Spring Creek Bonebed humeri showing bone microstructure.

<!--[if !msEquation]--> <!--[if !vml]--> <!--[endif]--><!--[endif]--> (A) Thin section of a humerus (UALVP 60539) showing the typical bone microstructure of humeri from the Spring Creek Bonebed, as described in the text. Scale bar = 1 mm. White arrows: 1, cancellous bone; 2, reticular bone; 3, plexiform bone; 4, laminar bone; 5, Haversian bone. (B) Laminar bone from UALVP 60533. Scale bar = 500 µm. (C) Reticular bone from UALVP 60535. Scale bar = 500 µm. (D) Plexiform bone from UALVP 60535. Scale bar = 500 µm. (E) Haversian reconstruction from UALVP 60539. Scale bar = 500 µm.

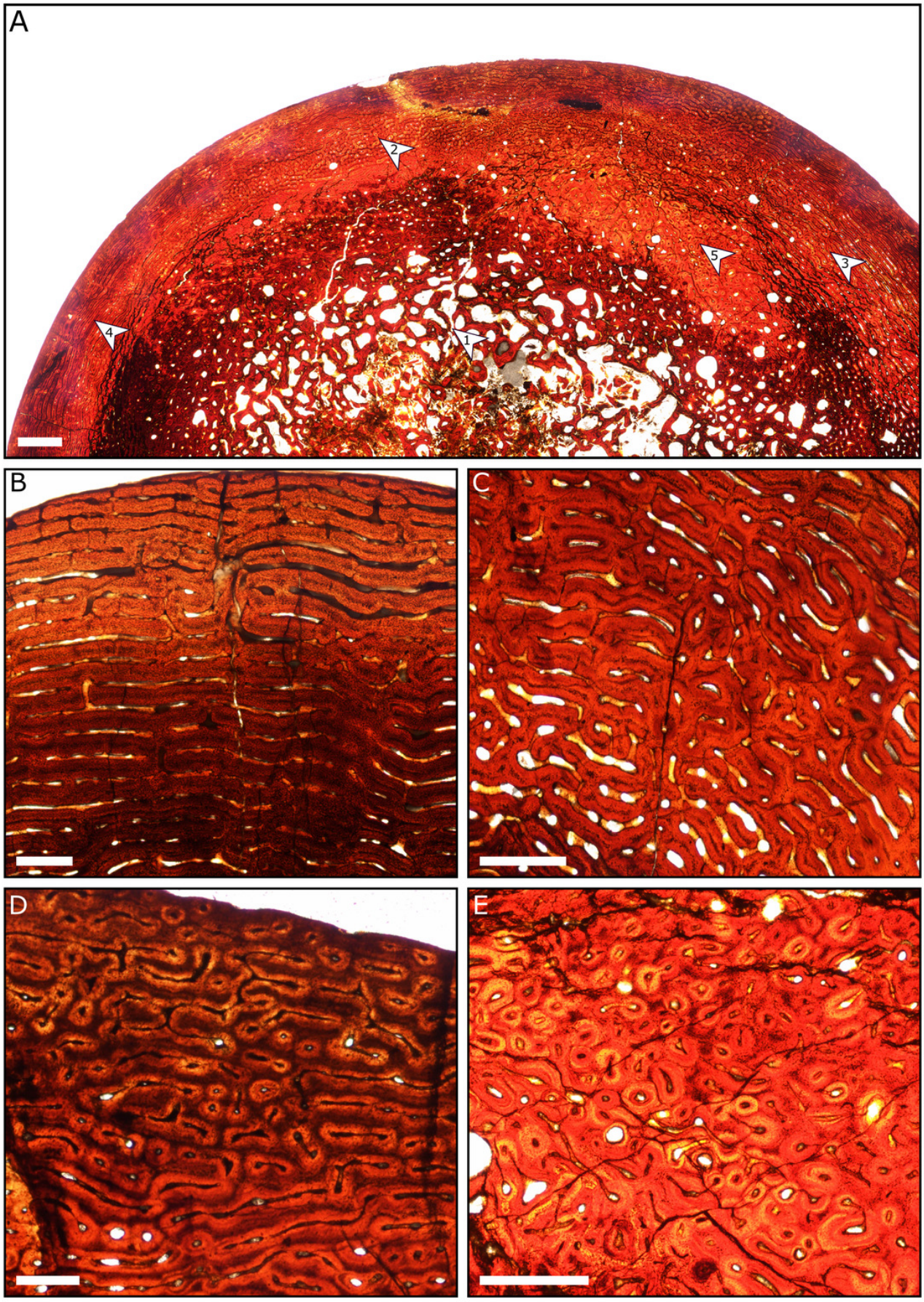
A
1
2
3
4
5
B
C
D
E

Figure 9

Examples of bone modification from the Spring Creek Bonebed.

(A) Unhealed parallel toothmarks (white arrows) on the lateral surface of the left dentary (UALVP 59907) interpreted as post mortem scavenging. (B) Pathology (margin indicated by white arrows) on the lateral surface of the supra-acetabular process (sa) from an incomplete ilium (UALVP 60540). (C) Example of paralell striae on the diaphysis of a fibula (UALVP 59982).

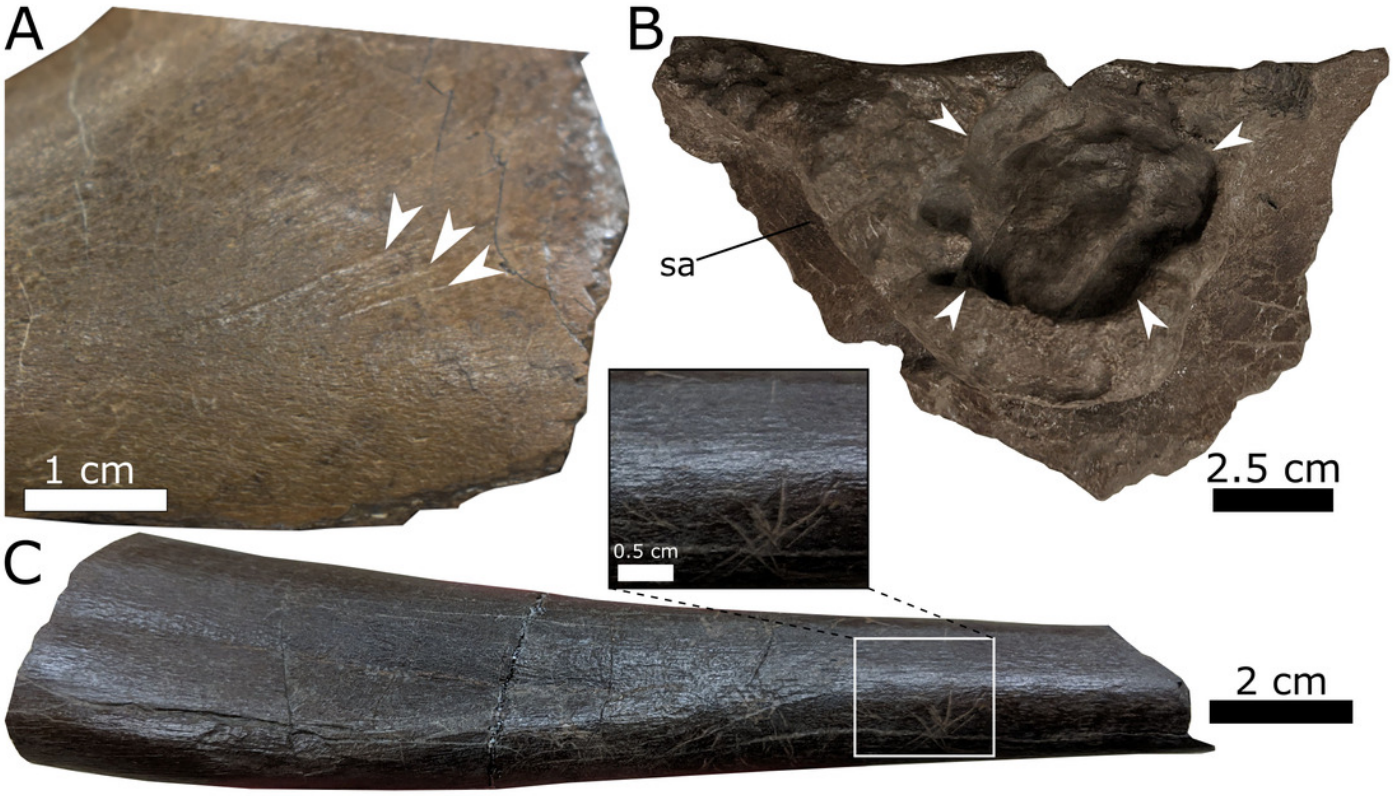

Figure 10

Biostratigraphy and palaeobiogeography of temporally and spatially proximate Lambeosaurinae from Alberta, Canada, Montana, USA, and Mexico.

(A) Biostratigraphic distribution of Lambeosaurinae across strata from northwestern (Fanti & Catuneanu, 2009; this study) and southern Alberta, Canada (Mallon et al., 2012; Eberth et al., 2013; Eberth & Kamo, 2020), Montana, USA (Horner & Currie, 1994; Campbell et al., 2019), western and northeastern Mexico (Lucas & Sullivan, 2006; Gates et al., 2007; Prieto-Márquez et al., 2012; Fowler, 2017). The Wapiti and Horseshoe Canyon formations are subdivided into units and members, respectively. Grey strata represent marine formations. The dashed error ranges for the Spring Creek lambeosaurines represents a temporal range within Unit 3, between the Pipestone Creek Bonebed (~73.5 Ma; Currie et al., 2008b) and the basal-most Horseshoe Canyon Formation (~74.4 Ma; Eberth & Braman, 2012). (B) Paleobiogeographical distribution of Lambeosaurinae across Montana, USA, Alberta, Canada, and Mexico (Lull & Wright, 1942; Horner & Currie, 1994; Evans & Reisz, 2007; Evans et al., 2007; Gates et al., 2007; Evans et al., 2009; Evans, 2010; Prieto-Márquez et al., 2012). The silhouette of the Spring Creek lambeosaurine and *Magnapaulia laticaudus* were created by Scott Hartman and Dmitry Bogdanov, respectively. Both were vectorized by T. Michael Keesey and used under the creative commons attribution 3.0 unported license (https://creativecommons.org/licenses/by/3.0/). The remaining silhouettes were used and modified under the public domain dedication 1.0 license. All silhouettes were sourced from www.phylopic.org .

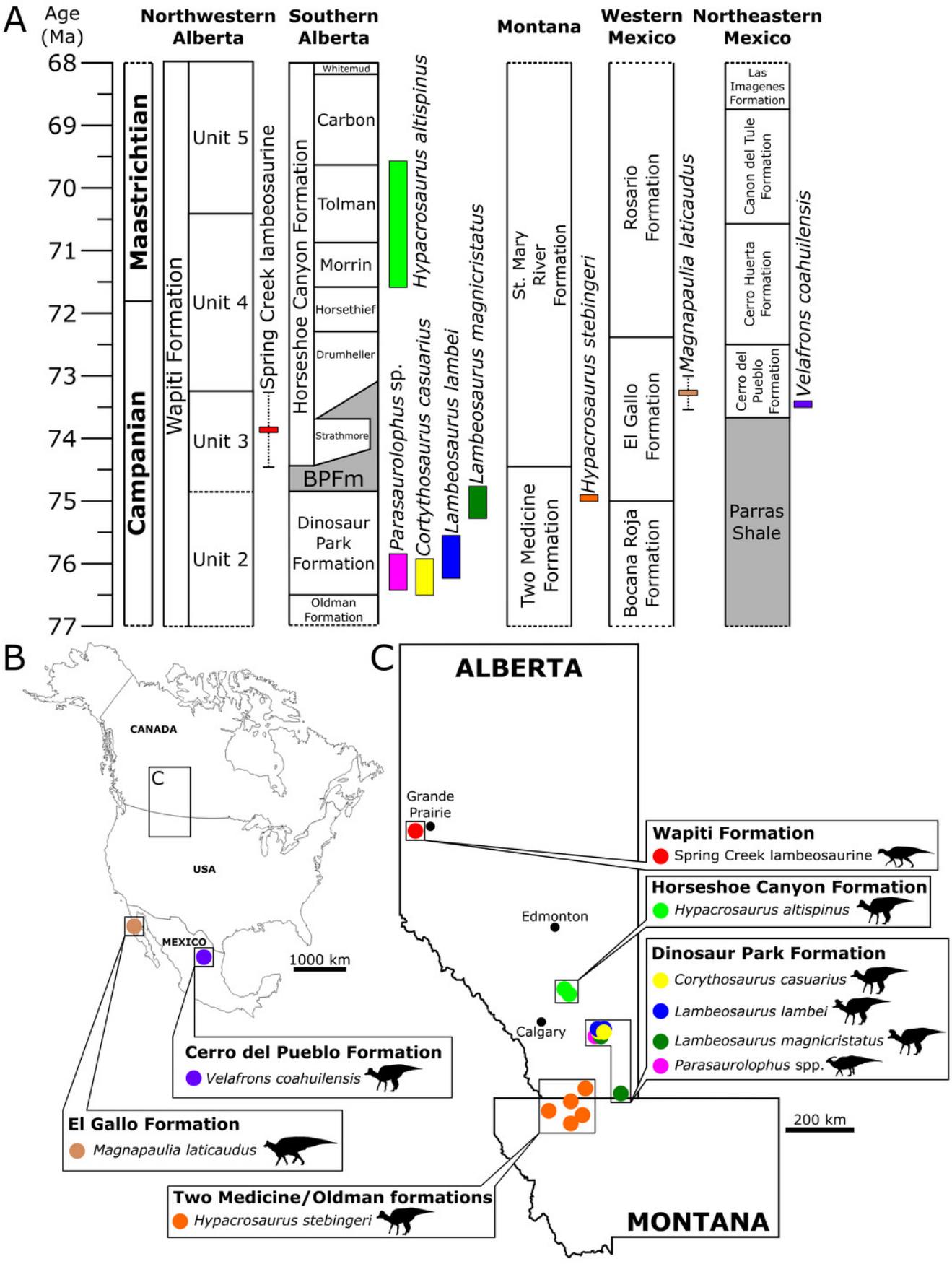
A
Age (Ma)
Northwestern Alberta
Southern Alberta
Montana
Western Mexico
Northeastern Mexico
68
69
70
71
72
73
74
75
76
77
Maastrichtian
Campanian
Wapiti Formation
Unit 5
Unit 4
Unit 3
Unit 2
Spring Creek lambeosaurine
Horseshoe Canyon Formation
Whitemud
Carbon
Tolman
Morrin
Horsethief
Drumheller
Strathmore
BPFm
Dinosaur Park Formation
Oldman Formation
Hypacrosaurus altispinus
Parasaurolophus sp.
Corythosaurus casuarius
Lambeosaurus lambei
Lambeosaurus magnicristatus
St. Mary River Formation
Two Medicine Formation
Hypacrosaurus stebingeri
Rosario Formation
El Gallo Formation
Bocana Roja Formation
Magnapaulia laticaudus
Las Imagenes Formation
Canon del Tule Formation
Cerro Huerta Formation
Cerro del Pueblo Formation
Parras Shale
Velafrons coahuilensis
B
CANADA
USA
MEXICO
C
1000 km
C
ALBERTA
Grande Prairie
Edmonton
Calgary
Wapiti Formation
Spring Creek lambeosaurine
Horseshoe Canyon Formation
Hypacrosaurus altispinus
Dinosaur Park Formation
Corythosaurus casuarius
Lambeosaurus lambei
Lambeosaurus magnicristatus
Parasaurolophus spp.
Cerro del Pueblo Formation
Velafrons coahuilensis
El Gallo Formation
Magnapaulia laticaudus
Two Medicine/Oldman formations
Hypacrosaurus stebingeri
200 km
MONTANA